

LMSC-D633363  
DECEMBER 1978

12

LEVEL

# A FUNDAMENTAL STUDY OF FLOW AND FRACTURE IN BERYLLIUM

FINAL REPORT

ARO PROJECT P-13387-MS

CONTRACT DAAG29-76-C-0051

DISTRIBUTION STATEMENT A

Approved for public release  
Distribution Unlimited

DDC

APR 1 1979

F

AD A0 651 50

DDC FILE COPY



**LOCKHEED**

PALO ALTO RESEARCH LABORATORY

LOCKHEED MISSILES & SPACE COMPANY, INC.

A SUBSIDIARY OF LOCKHEED CORPORATION  
PALO ALTO, CALIFORNIA

AX-000004 100  
P.000  
1.0

LMSC-D633363  
DECEMBER 1978

A

# A FUNDAMENTAL STUDY OF FLOW AND FRACTURE IN BERYLLIUM

FINAL REPORT

ARO PROJECT P-13387-MS

CONTRACT DAAG29-76-C-0051



**LOCKHEED**

PALO ALTO RESEARCH LABORATORY

LOCKHEED MISSILES & SPACE COMPANY, INC.

A SUBSIDIARY OF LOCKHEED CORPORATION  
PALO ALTO, CALIFORNIA

Unclassified

SECURITY CLASSIFICATION OF THIS PAGE (When Data Entered)

REPORT DOCUMENTATION PAGE		READ INSTRUCTIONS BEFORE COMPLETING FORM
1. REPORT NUMBER 1113387.2-MS	2. GOVT ACCESSION NO. 18 4101	3. RECIPIENT'S CATALOG NUMBER
4. TITLE (and Subtitle) A Fundamental Study of Flow and Fracture in Beryllium		5. TYPE OF REPORT & PERIOD COVERED Final Report 1 Jun 76 - 31 Oct 78
6. AUTHOR Donald Webster		7. PERFORMING ORG. REPORT NUMBER
8. PERFORMING ORGANIZATION NAME AND ADDRESS Lockheed Missiles & Space Company, Inc. Palo Alto, California		9. CONTRACT OR GRANT NUMBER(s) DAAG29-76-C-0051
10. CONTROLLING OFFICE NAME AND ADDRESS U. S. Army Research Office P. O. Box 12211 Research Triangle Park, NC 27709		11. REPORT DATE 11 Dec 78
12. MONITORING AGENCY NAME & ADDRESS (if different from Controlling Office) 101 LMMH/L623362		13. NUMBER OF PAGES 53
		14. SECURITY CLASS. (of this report) Unclassified
		15. DECLASSIFICATION/DOWNGRADING SCHEDULE
16. DISTRIBUTION STATEMENT (of this Report) Approved for public release; distribution unlimited.		
17. DISTRIBUTION STATEMENT (of the abstract entered in Block 20, if different from Report)		
18. SUPPLEMENTARY NOTES The view, opinions, and/or findings contained in this report are those of the author(s) and should not be construed as an official Department of the Army position, policy, or decision, unless so designated by other documentation.		
19. KEY WORDS (Continue on reverse side if necessary and identify by block number) Beryllium Powder Beryllium Alloys Beryllium Recrystallization Recrystallization Grain Boundaries Grain Boundary Fracture Grain Boundary Flow Grain Boundary Dislocations Beryllium Ingots		
20. ABSTRACT (Continue on reverse side if necessary and identify by block number) The effect of thermomechanical treatments on the grain size of HIP beryllium powder block and cast beryllium alloys has been studied. A grain-size controlled-fracture mode change has been observed in both powder-source and ingot-source beryllium. The mechanism of recrystallization in heavily deformed beryllium has been observed to be the in situ transformation of subgrains to grains by dislocation migration from grain interiors to grain boundaries. Beryllium which has been cold-worked and partly recrystallized to form some very fine grains was found to be much tougher than either unworked material or fully recrystallized material and approached the toughness of high-		

## 20. ABSTRACT CONTINUED

strength aluminum alloys. In upset-forged beryllium where the texture is similar to that of hot-pressed block, strength, ductility, and toughness were improved by partial recrystallization. The enhancement of ductility and toughness are believed to be a result of grain-boundary sliding in the regions where very fine grains occur. Transmission electron microscopy has been used to show the early stages of grain-boundary fracture and the grain-boundary dislocation structure preceding fracture. This work indicates that the use of rapidly cooled beryllium powder rather than impact ground powder would allow a further increase in ductility and toughness.

## SUMMARY

The effect of thermomechanical treatments on the grain size of HIP beryllium powder block and cast beryllium alloys has been studied. A grain-size controlled-fracture mode change has been observed in both powder-source and ingot-source beryllium. The mechanism of recrystallization in heavily deformed beryllium has been observed to be the in situ transformation of subgrains to grains by dislocation migration from grain interiors to grain boundaries. Beryllium which had been cold-worked and partly recrystallized to form some very fine grains was found to be much tougher than either unworked material or fully recrystallized material and approached the toughness of high-strength aluminum alloys. In upset-forged beryllium where the texture is similar to that of hot-pressed block, strength, ductility, and toughness were improved by partial recrystallization. The enhancement of ductility and toughness are believed to be a result of grain-boundary sliding in the regions where very fine grains occur. Transmission electron microscopy has been used to show the early stages of grain-boundary fracture and the grain-boundary dislocation structure preceding fracture. This work indicates that the use of rapidly cooled beryllium powder rather than impact ground powder would allow a further increase in ductility and toughness.

# CONTENTS

Section		Page
	SUMMARY	ii
	ILLUSTRATIONS	iv
1	OBJECTIVE	1
2	BACKGROUND	2
3	MATERIALS	3
4	EXPERIMENTAL TECHNIQUE	4
5	RESULTS AND DISCUSSION	5
	5.1 Grain Refinement By Recrystallization	5
	5.2 Fracture Mode Transition	17
	5.3 Microstructural Observations of the Initial Stages of Fracture	28
	5.4 Impact Resistance	39
	5.5 Tensile Properties	46
	5.6 Discussion	49
6	CONCLUSIONS	52
7	REFERENCES	53

## ILLUSTRATIONS

Figure		Page
1	Effect of Degree of Rolling Reduction on the Grain Size of High-Purity Cast Beryllium (EFI) Rolled With Intermediate Recrystallizing Anneals	6
2	Effect of Degree of Rolling Reduction on the Grain Size of Cast Beryllium Containing 0.13% Cr Rolled With Intermediate Recrystallizing Anneals	7
3	Effect of Degree of Rolling Reduction on the Grain Size of High-Purity Cast Beryllium (EFI) Rolled Without Intermediate Recrystallizing Anneals	9
4	Effect of Degree of Rolling Reduction on the Grain Size of Cast Beryllium Containing 0.19% Ti Rolled Without Intermediate Recrystallization Anneals	10
5	Effect of Annealing Time and Temperature on the Grain Size of High-Purity Cast Beryllium Rolled 93% After Upset Forging	11
6	Effect of Annealing Time and Temperature on the Grain Size of Cast Beryllium 0.13% Cr	12
7	Isothermal Grain Growth at 977 K for EFI and Be 0.13% Cr Alloys	13
8	Optical Micrograph of EFI, Rolled 96% and Annealed 977 K 5 Minutes	14
9	Optical Micrograph of Be 0.13% Cr Rolled 96% and Annealed 977 K, 5 Minutes	15
10	Transmission Electron Micrograph of EFI, Rolled 96% and Annealed 977 K, 1 Minute	16
11	Transmission Electron Micrograph of EFI Rolled 96% and Annealed 977 K, 1 Minute	18
12	Transmission Electron Micrograph of Be 0.13% Cr Rolled 90% and Annealed at 977 K, 5 Minutes	19
13	Scanning Electron Micrograph of EFI Rolled 96%, Annealed 977 K, 5 Minutes, and Fractured at Room Temperature	21
14	Replica of Fracture Surface of Cast Be 0.19% Ti, Reduced 90% by Rolling and Partially Recrystallized at 977 K for 5 Minutes	22

		Page
15	Replica of Fracture Surface of HIP 1.56% BeO (RR243) Extruded 10:1 at 1033 K and Annealed for 1 hr at 1144 K	23
16	Replica of Fracture Surface of HIP Be, 0.70 BeO, Upset-Forged 1033 K, Reduced 75% by Rolling at 922 K, and Annealed at 977 K for 10 Minutes	24
17	Higher Magnification View of Sample in Fig. 16 Showing a Region of Fine Intergranular Fracture	25
18	Grain-Size Controlled Fracture Mode Transition for High-Purity Ingot Source Beryllium (EFI), Upset-Forged and Annealed at Either 1061 K or 1116 K	26
19	Grain-Size Controlled Fracture Mode Transition for High-Purity Ingot Source Beryllium (EFI), Warm-Rolled 96% and Annealed at Various Temperatures	27
20	The Effect of Temperature on the Grain-Size Controlled Fracture Mode Transition for High-Purity Upset-Forged, Ingot Source Beryllium (EFI)	29
21	Grain-Size Controlled Fracture Mode Transition for High-Purity HIP Power Block (BOP 32) After Upset-Forming and Warm-Rolling	30
22	Grain-Size Controlled Fracture Mode Transition for High-Purity HIP Beryllium RR243 After Extrusion and Annealing at Various Temperatures	31
23	Grain-Size Controlled Fracture Mode Transition for High-Purity "As-HIP" Beryllium Block (BOP 12 and BOP 22)	32
24	Transmission Electron Micrograph of Cast Be 0.10% Ti, Warm-Rolled 96%, Annealed 977 K 10 Minutes, and Then Cold-Rolled 15%	33
25	Transmission Electron Micrograph of High-Purity Powder Source Beryllium Alloy BOP 32, Upset-Forged, Rolled 75%, and Annealed 977 K 10 Minutes	35
26	Transmission Electron Micrograph of Be 0.7% BeO (BOP 32), Upset-Forged, Rolled 75% at 922 K, Partially Recrystallized for 1 hr at 977 K, and Reduced 10% by Cold-Rolling	36
27	High-Voltage (650 kV) Electron Transmission Micrograph of a Relatively Thick Foil of BOP 32, 0.7% BeO, Upset-Forged and Rolled 75% at 922 K, Partially Recrystallized at 977 K for 5 Minutes, and Then Reduced 10% at Room Temperature	37

Figure		Page
28	Transmission Electron Micrograph of BOP 32, 0.7% BeO, Upset-Forged and Rolled 75% at 922 K, Partially Recrystallized 977 K 1 hr, and Deformed by Rolling 10% at Room Temperature	38
29	Transmission Electron Micrograph of EFI Polled 96%, Annealed 977 K 1 hr, and Cold-Rolled 14%	40
30	Impact Toughness of Ingot Source Ee 0.5% V, After Various Thermomechanical Treatments	41
31	Impact Toughness of High-Purity HIP Beryllium After Extrusion and Annealing	42
32	Impact Toughness of High-Purity HIP Beryllium With Two Levels of BeO After Extrusion and Annealing	43
33	Impact Toughness of High-Purity HIP Beryllium With Two Levels of BeO After Extension and Annealing	44
34	Impact Toughness of High-Purity HIP Beryllium Block (BOP 32) After Upset-Forging and Warm-Rolling	45
35	Impact Transition Temperature for High-Purity HIP Beryllium (BOP 18) Extruded and Partially Recrystallized	47
36	The Effect of Grain Size on the Charpy Impact Energy of a Variety of Partially Recrystallized Beryllium Products	48
37	The Effect of Annealing Temperature on the Strength, Ductility, and Toughness of Upset-Forged Beryllium	51

Section 1  
OBJECTIVE

The objective of this program was to develop an understanding of the fundamental flow and fracture mechanism in beryllium. A specific objective of this program was to indicate how new mechanisms of flow and fracture could be utilized to overcome beryllium's low toughness.

## Section 2 BACKGROUND

Although modern beryllium has the highest structural efficiency of any material or composite, its use has been restricted by low ductility and toughness. In the last 5 years, the ductility of beryllium has been dramatically increased so that 6-percent elongation in all directions of a semicommercial, hot isostatically pressed, low oxide (0.5%) block can be produced routinely (Ref. 1). Still higher values of 13-percent elongation in virtually nontextured upset forgings of the same material have been produced experimentally (Ref. 2) and recent Russian work (Ref. 3) using upset forging of high-purity cast material has enabled three-dimensional tensile elongation of 22 percent to be obtained. For most structures, this degree of tensile elongation is more than adequate to permit designs that can utilize the full strength of the beryllium. At this stage, beryllium compares favorably in its mechanical properties with other engineering alloys in all aspects other than its resistance to impact shocks in the presence of a stress concentration. This condition is simulated experimentally by charpy impact testing which is used on this program to evaluate the effects of microstructural and mechanistic changes on toughness.

### Section 3 MATERIALS

Two basic types of beryllium were used on this program:

- (1) High-purity powder products formed from electrolytic flake and then hot isostatically pressed (HIP) by Kawecki Beryllco Industries (KBI)
- (2) Vacuum-cast ingots 2- to 3-in. -diameter containing small (0.1-0.5%) addition of titanium, vanadium, or chromium plus a high-purity vacuum-cast ingot (EFI) containing no alloying additions

Table 1  
CHEMICAL COMPOSITION OF MATERIALS

Alloy	Form	Composition PPM									
		BeO	Mg	Si	Al	Fe	C	Ti	Ni	Cr	V
EFI	Ingot	40	10	100	90	110	296	N. D.	N. D.	N. D.	N. D.
Be-Ti	Ingot	N. D.	20	380	670	290	520	1900	130	40	80
Be-Cr	Ingot	N. D.	10	70	20	140	360	N. D.	N. D.	1300	N. D.
Be-V	Ingot	N. D.	10	400	660	250	550	150	170	30	5700
BOP 11	HIP Block	5,100	36	90	35	146	220	N. D.	185	N. D.	N. D.
BOP 12	HIP Block	4,800	26	90	30	146	220	N. D.	195	N. D.	N. D.
BOP 16	HIP Block	5,000	50	110	35	140	130	N. D.	41	N. D.	N. D.
BOP 18	HIP Block	5,100	32	150	30	250	370	N. D.	260	N. D.	N. D.
BOP 22	HIP Block	5,300	37	70	33	180	180	N. D.	360	N. D.	N. D.
BOP 30	HIP Block	6,700	41	120	35	185	280	N. D.	265	N. D.	N. D.
BOP 32	HIP Block	7,000	35	140	33	178	210	N. D.	250	N. D.	N. D.
RR 243	HIP Block	15,600	30	36	16	550	200	N. D.	N. D.	16	N. D.

N. D. Not Determined.

#### Section 4 EXPERIMENTAL TECHNIQUE

All beryllium samples were canned in mild steel prior to forging extrusion or rolling to prevent surface cracking. Upset forging was carried out at 1033 K (1400°F), rolling at either 1033 K or 922 K (1200°F) and extrusion (10:1 reduction) at 894 K (1150°F).

Fractographic examination was performed by scanning electron microscopy for coarse grained ( $> 50 \mu\text{m}$ ) samples and by transmission electron microscopy of shadowed replicas for finer-grained materials.

Direct transmission electron microscopy of the beryllium was conducted after electropolishing in a solution containing 82% ethylene glycol, 5%  $\text{H}_2\text{O}$ , 9%  $\text{HNO}_3$ , 2%  $\text{H}_2\text{SO}_4$ , and 2%  $\text{HCl}$ . Both conventional (120 kV) and high-voltage (650 kV) electron microscopes were utilized to examine the electropolished foils.

Charpy specimens for impact testing were made with the rounded notch, 1-mm radius and 1.5-mm deep conventionally used with beryllium. The surface was etched before testing to remove 0.1 mm of potentially damaged surface material. The specimens were tested on a 24-ft/lb impact machine.

Upset forging was conducted as described previously (Ref. 2).

## Section 5 RESULTS AND DISCUSSION

### 5.1 GRAIN REFINEMENT BY RECRYSTALLIZATION

Grain refinement in beryllium, as in most other metals, confers property improvements such as higher toughness and tensile elongation (Ref. 1) together with higher strength (Ref. 4), but there are limitations to how far this refinement can be taken. In powder block beryllium, the grain size is similar to that of the input powder and any degree of grain refinement can be obtained by reducing the powder size. However, this increases the surface area of the powder and hence the oxide level. This counteracts the benefits of grain refinement on toughness and ductility, and optimum properties are observed when the grain size is approximately  $10\text{ }\mu\text{m}$ . In cast beryllium where oxide is not normally present in sufficient quantities to act as a grain refiner, it is very difficult to produce a recrystallized grain size less than  $30\text{ }\mu\text{m}$  even in sheet. An alternative method of grain refinement investigated in this program is to use intermetallic compounds of titanium, vanadium, and chromium to act as grain refiners in cast and wrought beryllium.

Two types of thermomechanical treatment were conducted to determine which was most effective in producing grain refinement. In the first type, the beryllium was deformed about 20 percent and fully recrystallized at the minimum temperature at which this could be accomplished. The recrystallized material was then rolled to about 40 percent and recrystallized again. This process was repeated for 90- and 96-percent reductions. The grain size was reduced at each step as shown in Fig. 1 for high-purity beryllium (EFI) and Fig. 2 for the 0.19-percent Ti alloy.

The initial "as-cast" grain size was taken as the dendrite width which is about ten times smaller than the average dendrite length in both cases.

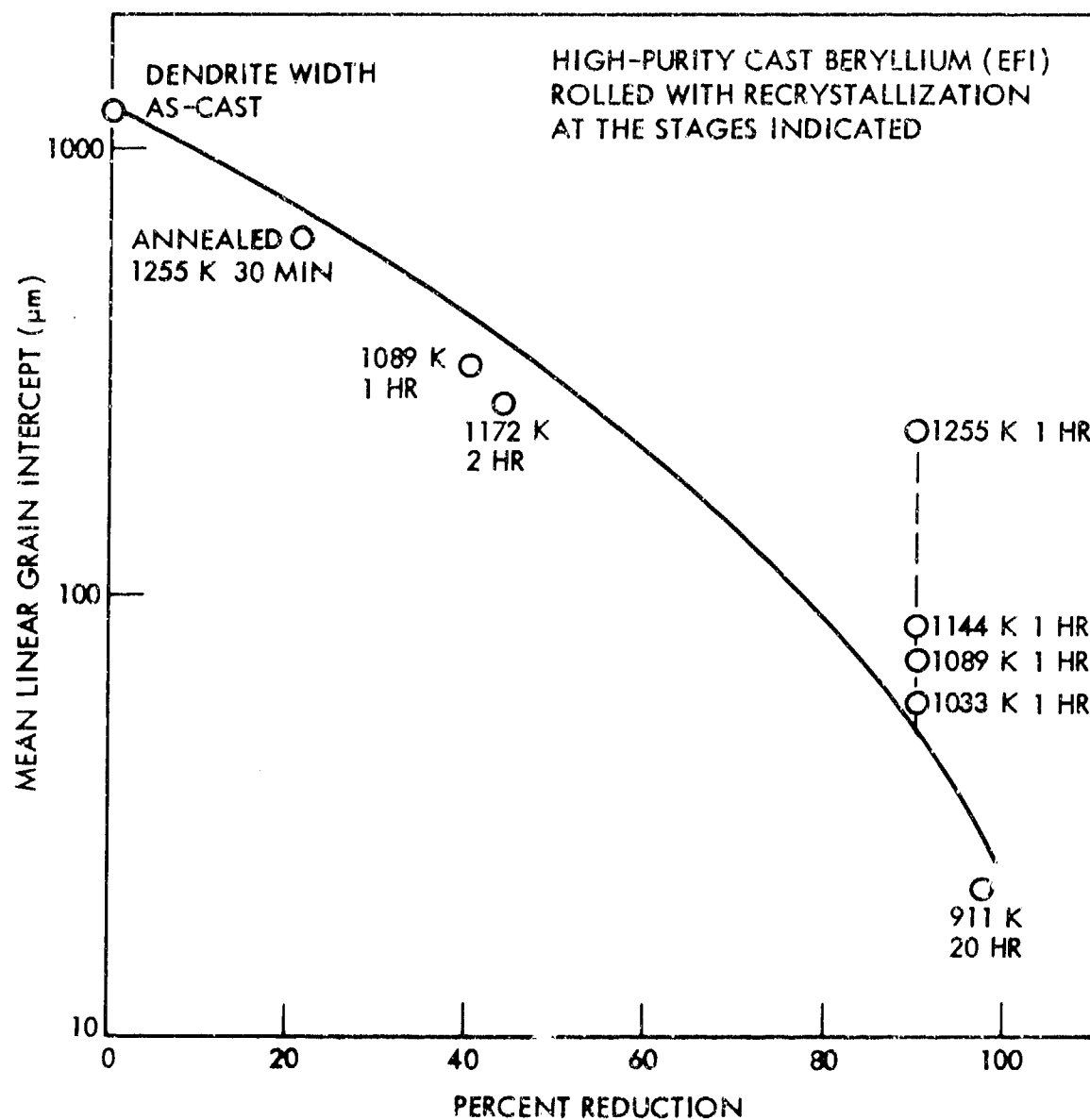


Fig. 1 Effect of Degree of Rolling Reduction on the Grain Size of High-Purity Cast Beryllium (EFI) Rolled With Intermediate Recrystallization Anneals

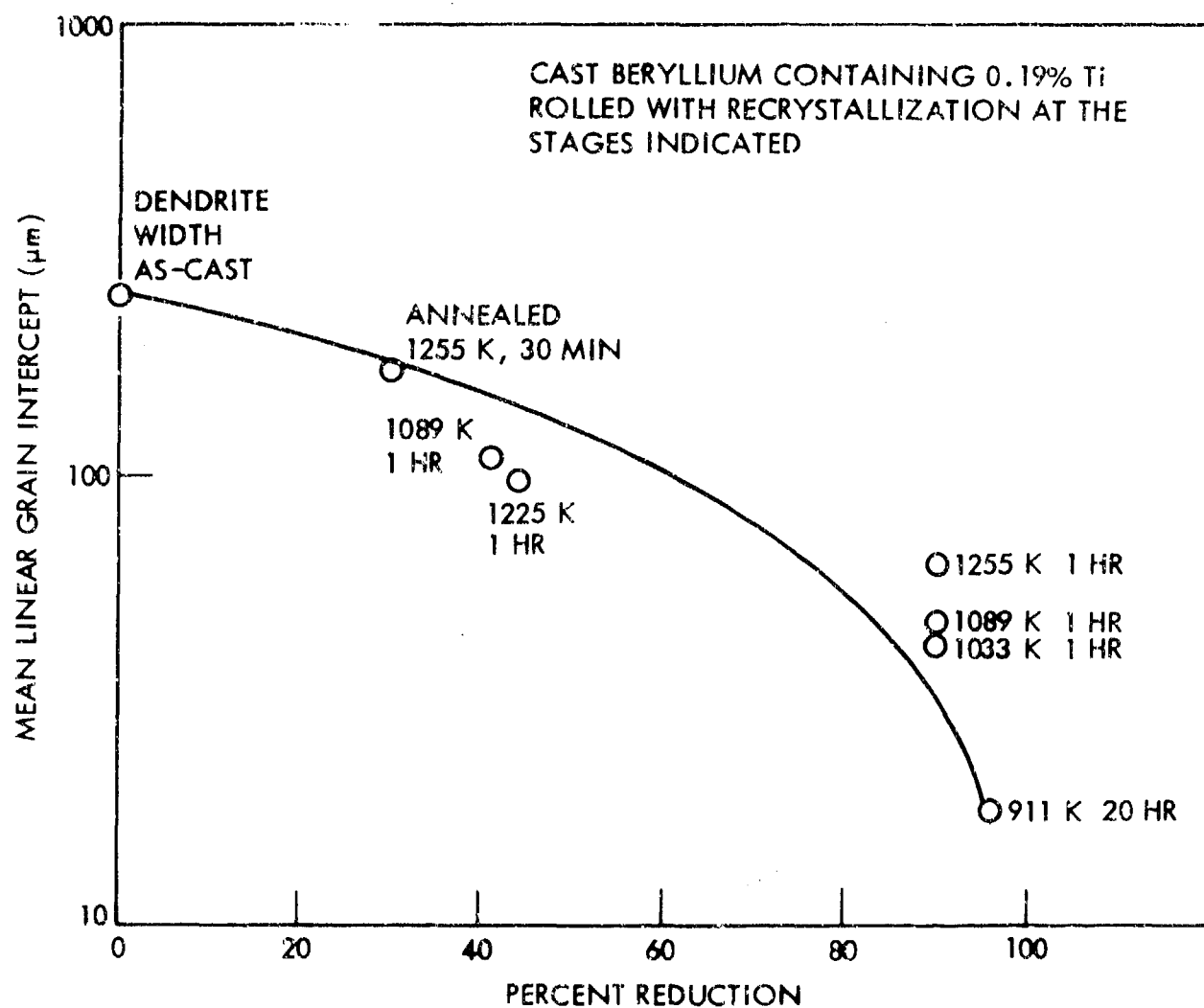


Fig. 2 Effect of Degree of Rolling Reduction on the Grain Size of Cast Beryllium Containing 0.13% Cr Rolled With Intermediate Recrystallizing Anneals

In the second type of thermomechanical process, the specimens were rolled 90 or 96 percent before recrystallization anneals were performed. These results are shown in Figs. 3 and 4 for EFI and 0.19% Ti, respectively. A comparison of the two types of thermomechanical treatments shows that the direct reduction without interstage anneals is more effective for both materials in producing grain refinement. This result follows from an examination of the recrystallization mechanism as will be discussed below. The 0.19% Ti addition can be seen to produce grain refinement in both processes and also produces some refinement of the as-cast dendrite size.

Recrystallized grain sizes after upset forging and rolling are shown in Figs. 5 and 6 for EFI and a 0.13% Cr alloy. There appears to be no particular advantage to any particular temperature in terms of grain size, but annealing temperatures above 950 K produce fully recrystallized structures in less than 72 hr.

A more detailed study of the recrystallization of EFI and Be-0.13% Cr was conducted at 977 K (Fig. 7). The recrystallized grain size was measured in both alloys in the early stages of recrystallization when the structure was only partially recrystallized. Recrystallization is obviously retarded in the chromium alloy, probably by the intermetallic compounds.

In this alloy, grain growth is continuing in the recrystallized areas even though further nucleation of recrystallized grains is inhibited. The optical microstructure of EFI and Be 0.13% Cr after 5 min at 977 K is shown in Figs. 8 and 9, respectively. In both materials faint, ghostly "grains" can be seen inside what appears to be large unrecrystallized areas. These are actually subgrains in the process of transforming to grains. This process is revealed in more detail by transmission electron microscopy.

The subgrain structure of EFI in the vicinity of an original grain boundary after rolling 95 percent and annealing for 1 min at 977 K is shown in Fig. 10. Most of the subgrains have poorly defined boundaries and a high density of dislocations in the subgrain interiors. A few of the subgrains, such as those at A on the original grain boundary, have low

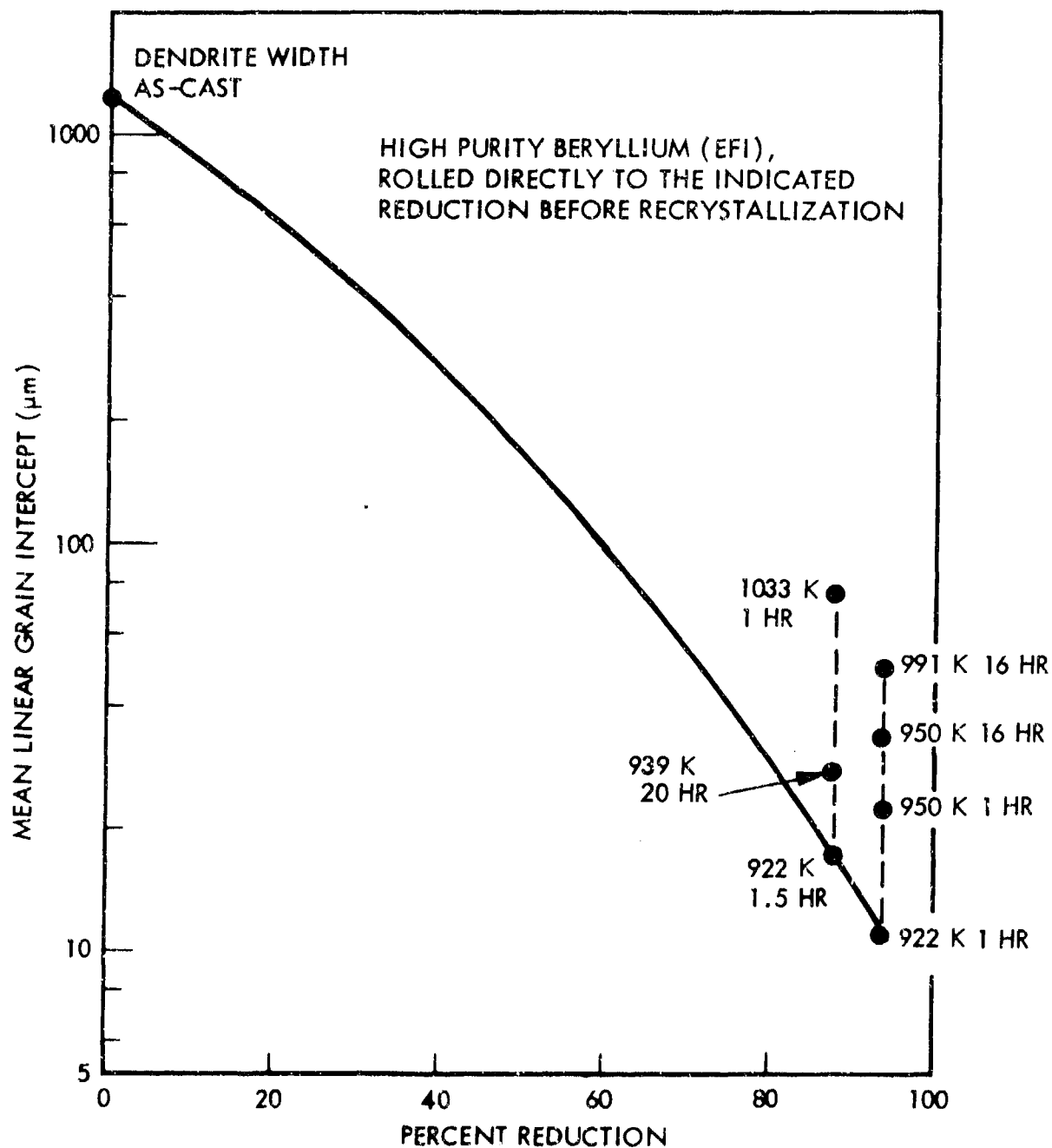


Fig. 3 Effect of Degree of Rolling Reduction on the Grain Size of High-Purity Cast Beryllium (EFI) Rolled Without Intermediate Recrystallizing Anneals

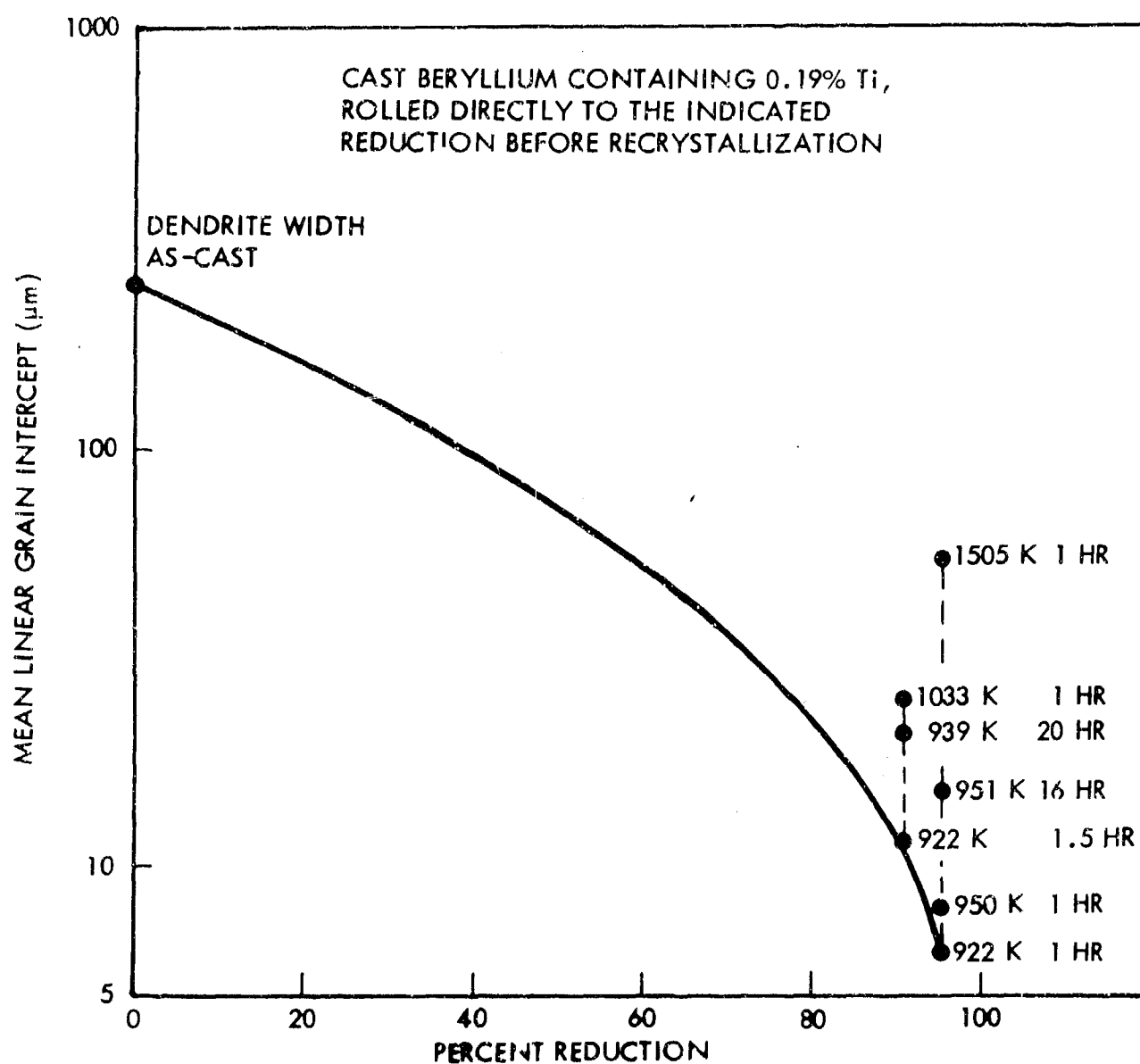
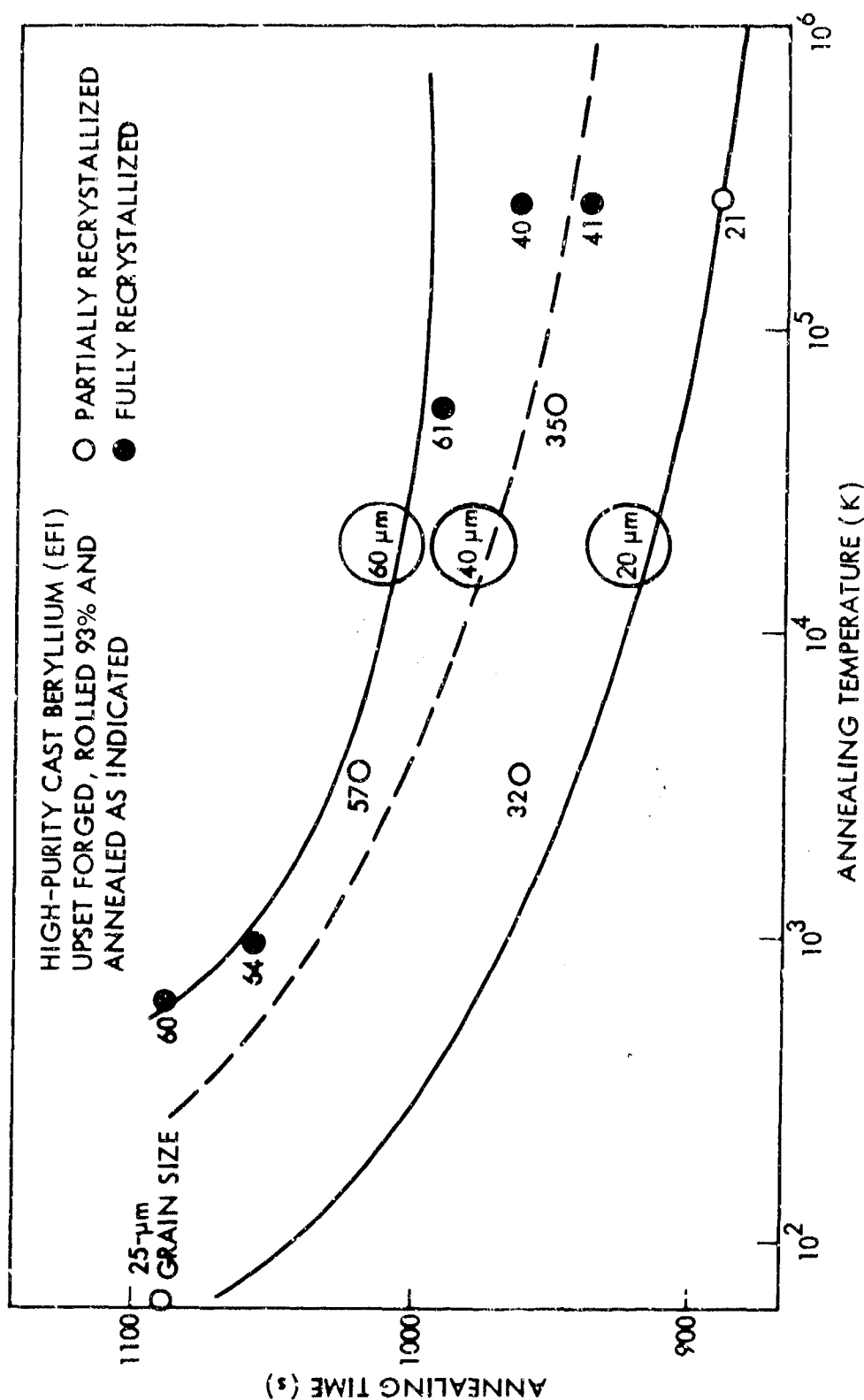


Fig. 4 Effect of Degree of Rolling Reduction on the Grain Size of Cast Beryllium Containing 0.19% Ti Rolled Without Intermediate Recrystallizing Anneals



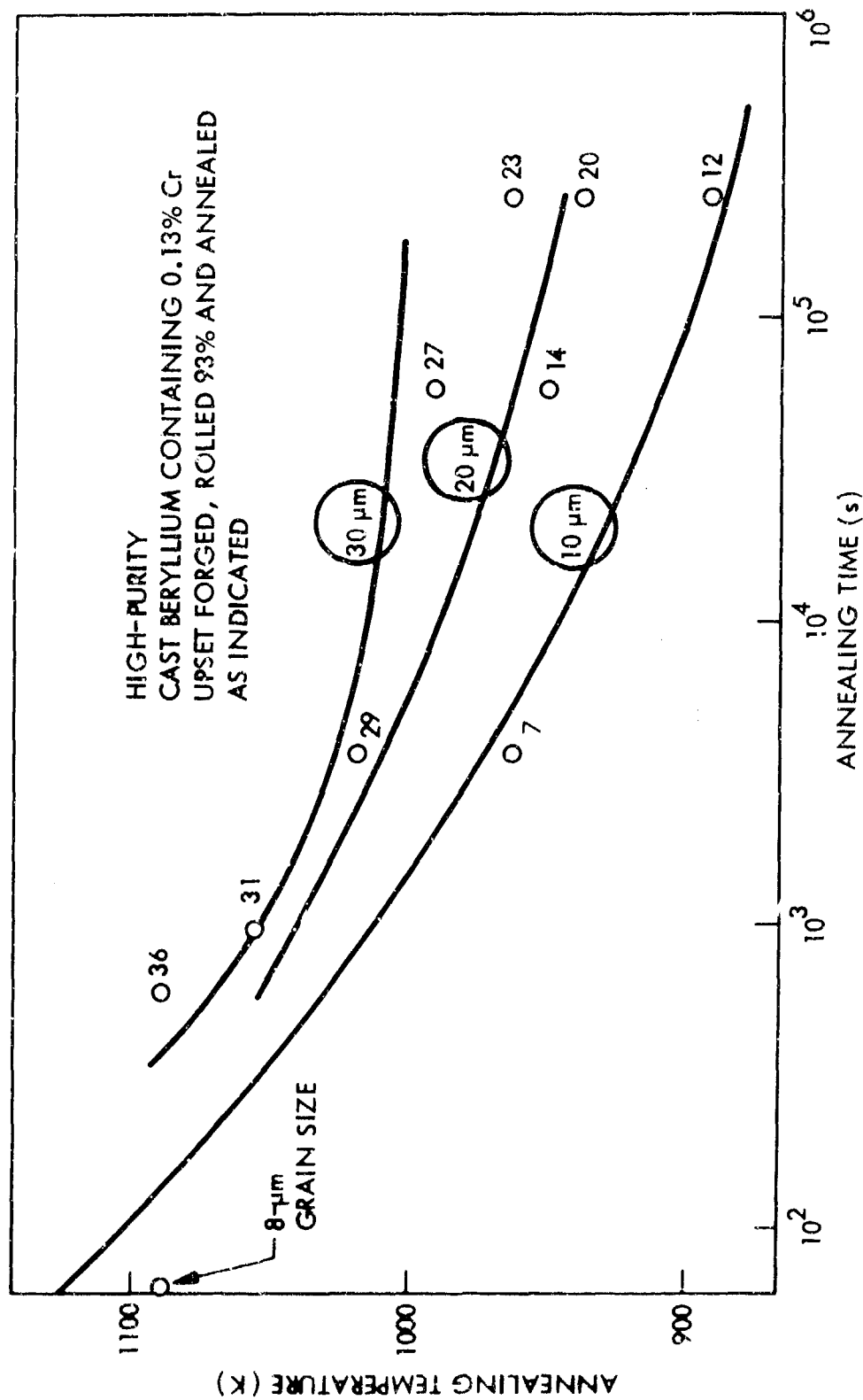


Fig. 6 Effect of Annealing Time and Temperature on the Grain Size of Cast Beryllium 0.13% Cr

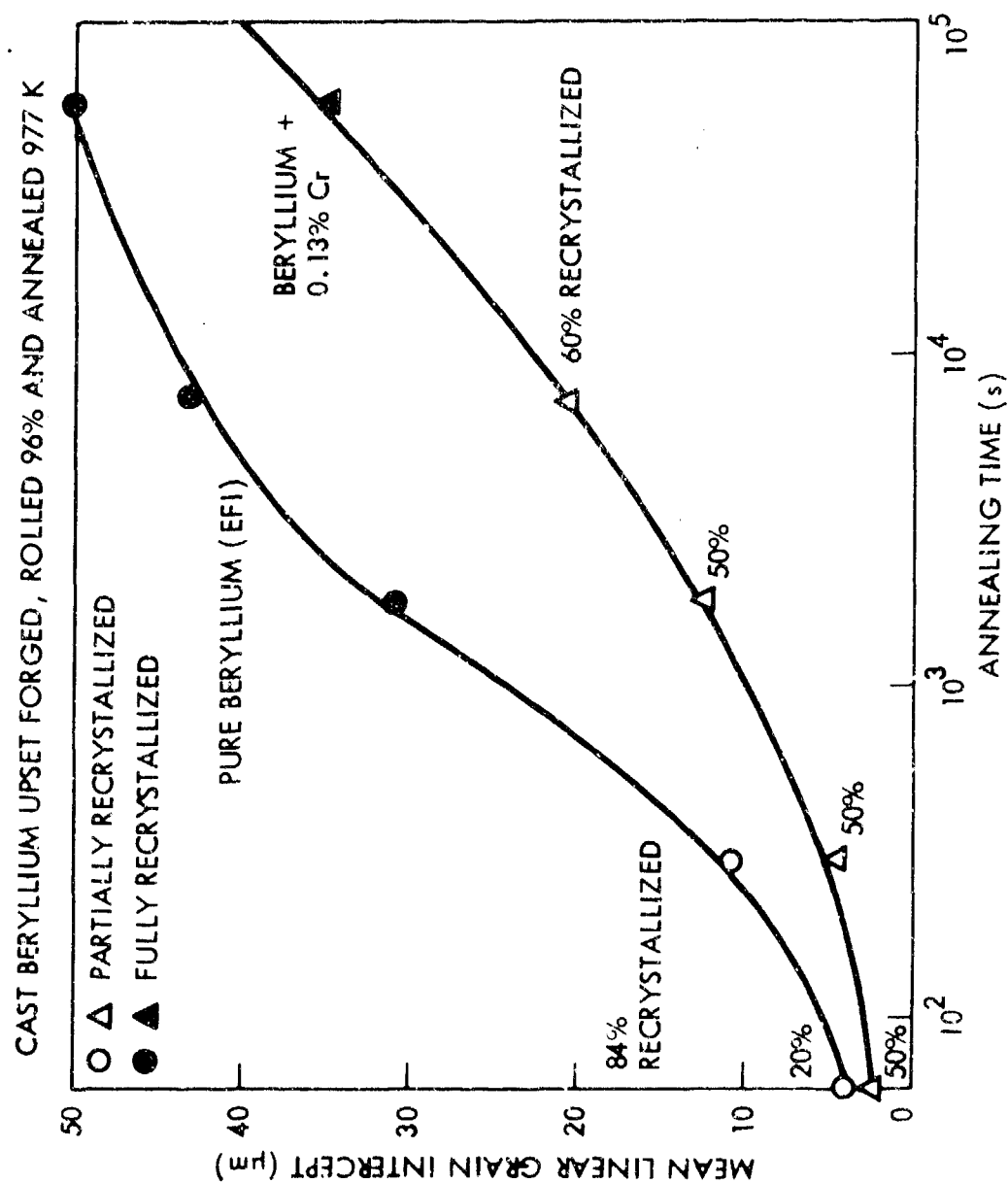


Fig. 7 Isothermal Grain Growth at 977 K for EFI and Be 0.13% Cr Alloys



Fig. 8 Optical Micrograph of EFL, Rolled 96% and Annealed 977 K, 5 Minutes. Faint 'ghostly' subgrains can be seen in some unrecrystallized areas. Magnification 200x



Fig. 9 Optical Micrograph of Be 0.13% Cr Rolled 96% and Annealed at 977 K, 5 Minutes. Magnification 200x



Fig. 10 Transmission Electron Micrograph of EET, Rolled 96% and Annealed 977 K, 1 Minute. Grains at A are almost recrystallized. Magnification 16,000x.

dislocation densities and may appear in polarized light to be the ghostly recrystallized grains described above for Figs. 8 and 9. In other areas of the same sample, the recrystallization process has progressed further as shown for grain A in Fig. 11 where the grain interior is dislocation-free and the boundaries are sharply defined. This grain would appear in polarized light to be fully recrystallized. A still later stage of recrystallization is shown in Fig. 12 which shows the Be 0.13% Cr alloy after 90-percent reduction and an anneal of 6 min at 977 K. This area shows a boundary between unrecrystallized subgrains and fully recrystallized grains with low dislocation densities and high-angle boundaries. The particle at A is a beryllium-chromium intermetallic with an associated deformation void. With continued annealing, the unrecrystallized subgrains in all the cast alloys are seen to transform gradually to recrystallized grains of the same size, although there is no definite point at which a grain can be said to be recrystallized by microscopic observation. However, there is a sharp transition in fracture mode during annealing which can be used to define the point at which the conversion from subgrain to grain is complete.

It follows from the above observation indicating the mechanism of recrystallization to be by subgrain transformation that the finest recrystallized grain size will result from the finest subgrain size. This subgrain size is found in most metals to be inversely proportional to the amount of cold work. This explains why in the two thermomechanical processes described above the finest grain size was produced when intermediate recrystallization steps, which would have reduced the total amount of cold work, were avoided. If the recrystallization mechanism had been by the growth of grain-boundary nuclei, then the gradual grain refinement produced by the intermediate recrystallization steps in the second process would have produced the finer grain size.

## 5.2 FRACTURE MODE TRANSITION

The normal fracture mode in both powder-source and ingot-source beryllium is cleavage. However, when the grain size is reduced below a certain critical value characteristic of each composition and method of manufacture, the fracture mode is by grain-boundary separation. Previous work (Ref. 2) has indicated grain-boundary sliding occurs prior to



Fig. 11 Transmission Electron Micrograph of EPI Rolled 96% and Annealed 977 K, 1 Minute. Grain at A is recrystallized. Magnification 8000x



Fig. 12 Transmission Electron Micrograph of Be 0.13% Cr Rolled 90% and Annealed at 977 K, 5 Minutes. Magnification 16,000x

fracture, and this additional slip mechanism may be responsible for the improved toughness and ductility of the fine-grained materials. The two fracture modes can be seen in Fig. 13 which shows the fracture surface of EFI after rolling 96 percent and partially recrystallizing for 5 min at 977 K. The unrecrystallized area, typified by A, shows cleavage with only minor perturbations in the fracture path across subgrain boundaries. The recrystallized areas, such as B, have grains which are about the same size as the subgrains but where fracture is completely intercrystalline. Similar fracture mode transitions are observed in partly recrystallized powder products (Figs. 14-17), but the transition is at finer-grain sizes than for cast and wrought products.

In Fig. 14, an isolated grain in a Be-O 19% Ti alloy has fractured in an intergranular manner while the surrounding grain fracture by cleavage. Figure 15 shows a mixture of intergranular fracture and cleavage fracture in a HIP powder product. BeO particles can be seen in the grain-boundary fracture surfaces. It should be noted that these fracture characteristics are easily seen in powder products using transmission electron microscopy of carbon replicas as shown in Figs. 14 through 17, but are very difficult to resolve with the lower contrast and resolution of the more commonly used scanning electron microscope. Figure 16 shows the fracture of a high-purity HIP powder product after upset forging, rolling, and partly recrystallizing. The fracture is mainly cleavage, but some areas of very fine intergranular fracture can be seen at A. Figure 17 shows an intergranular fracture area in this material at higher magnification.

The fracture mode transition temperature for high-purity ingot-source beryllium (EFI) after upset forging and annealing at two different temperatures is shown in Fig. 18. All grains under 35- $\mu$ m diameter fracture intergranularly. The largest grain size that fractures along the grain boundaries varies from 100  $\mu$ m in the sample annealed at 1061 K to 400  $\mu$ m in the sample annealed at 1116 K. This indicates that at the lower annealing temperature some excess dislocations remain inside the larger grains and encourage cleavage fracture. A similar fracture mode transition is seen when EFI, which has been reduced 96 percent by warm rolling, is annealed at 997 K, 1089 K, and 1172 K (Fig. 19). The main difference between the fracture of the relatively untextured upset-forged material and the highly textured rolled material is that the grain size at which all fracture is intergranular is displaced from 25  $\mu$ m to 4  $\mu$ m by the texture.

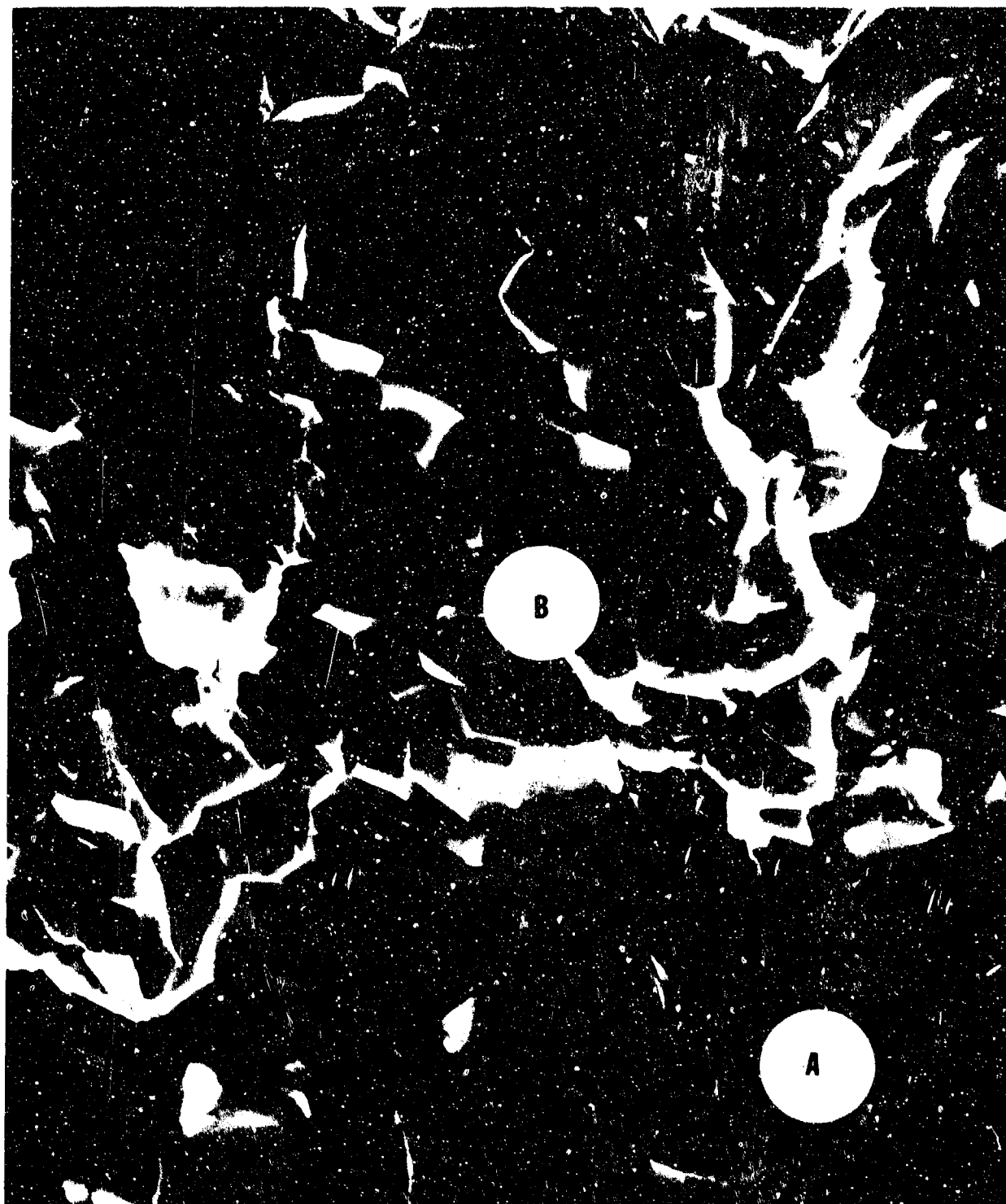


Fig. 13 Scanning Electron Micrograph of EFL Rolled 96% Al, Annealed 977 K, 5 Minutes and Fractured at Room Temperature. Subgrains at A Show Cleavage Fracture While Grains at B Show Intergranular Fracture. Magnification 1320x

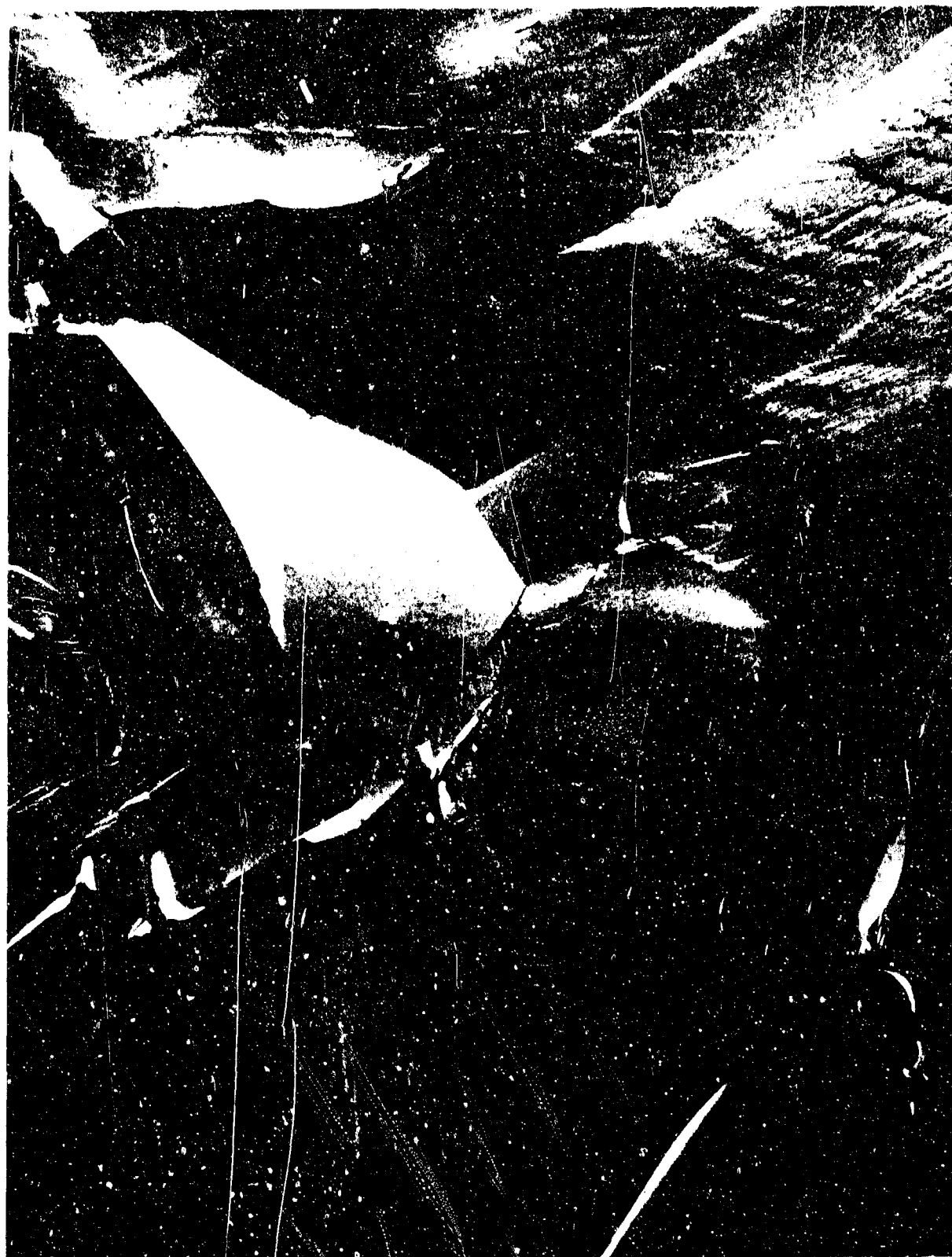


Fig. 14 Replica of Fracture Surface of Cast Be-0.19% Ti, Reduced 90% by Rolling and Partially Recrystallized at 977 K for 5 min. An isolated grain 3- $\mu$ m diameter has fractured along its boundary while the surrounding grains or subgrains have failed by transgranular cleavage. Magnification 24,000 $\times$



Fig. 15 Replica of Fracture Surface of HIP 1.56% BeO (RR243) Extruded 10:1 at 1033 K and Annealed for 1 hr at 1144 K. The fracture shows a mixture of fine (1-3  $\mu\text{m}$ ) intergranular failure and coarser transgranular cleavage failure. BeO particles up to about 200-nm diameter can be seen in the regions of intergranular separation. Magnification 15,000 $\times$ .

23

LOCKHEED PALO ALTO RESEARCH LABORATORY  
 LOCKHEED MISSILES & SPACE COMPANY, INC.  
 A SUBSIDIARY OF LOCKHEED AIRCRAFT CORPORATION



Fig. 16 Replica of Fracture Surface of HIP Be, 0.70 BeO, Upset-Forged 1033 K, Reduced 75% by Rolling at 922 K and Annealed at 977 K for 10 min. The structure mainly cleavage failure with isolated areas of fine intergranular fracture. Magnification 8000 $\times$ .



Fig. 17 Higher Magnification View of Sample in Fig. 16 Showing a Region of Fine Intergranular Fracture. BeO particles are visible on the grain-boundary surface. Magnification 60,000 $\times$

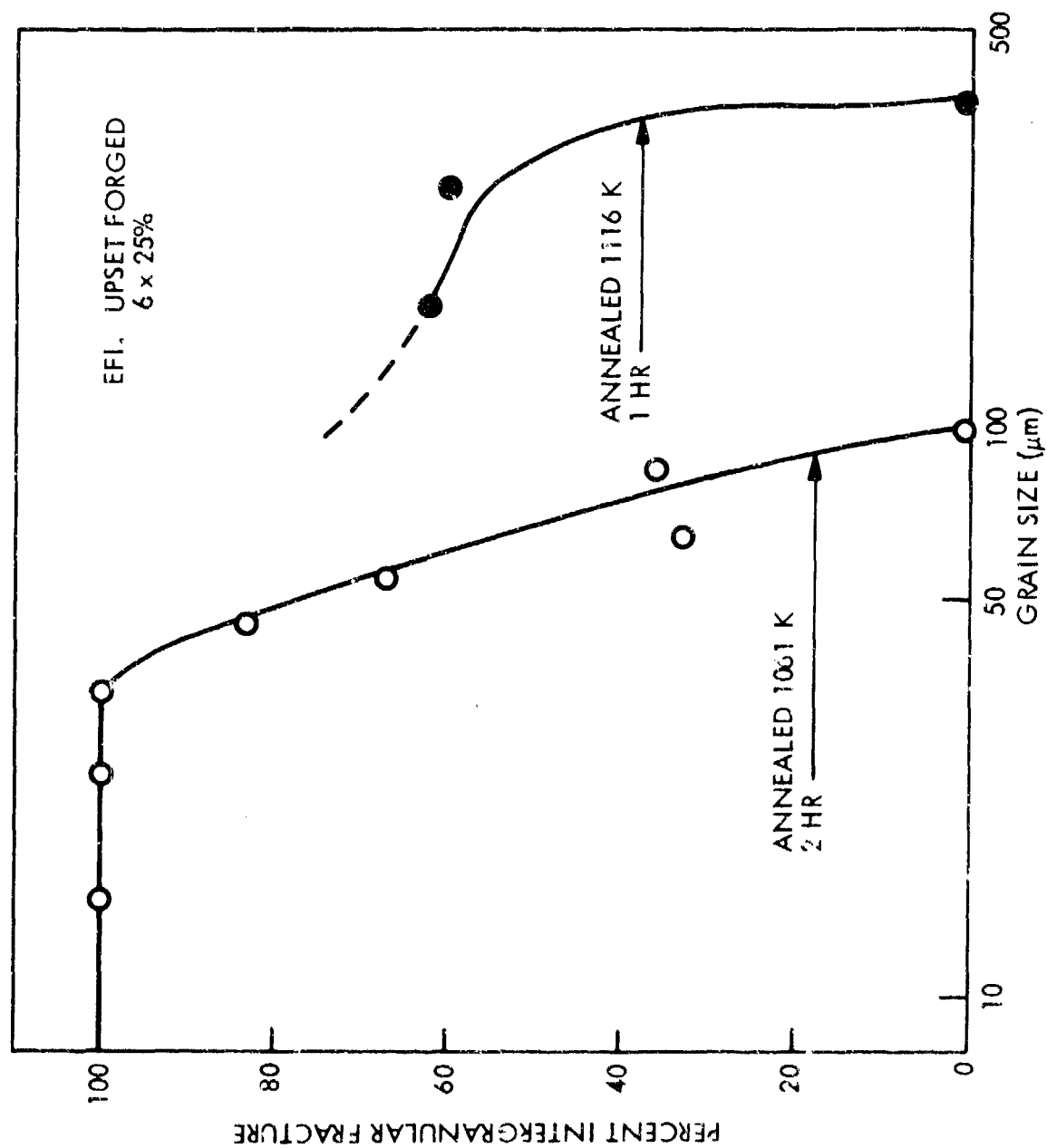


Fig. 18 Grain-Size Controlled Fracture Mode Transition for High-Purity Ingot Source Beryllium (EFL), Upset-Forged and Annealed at Either 1061 K or 1116 K

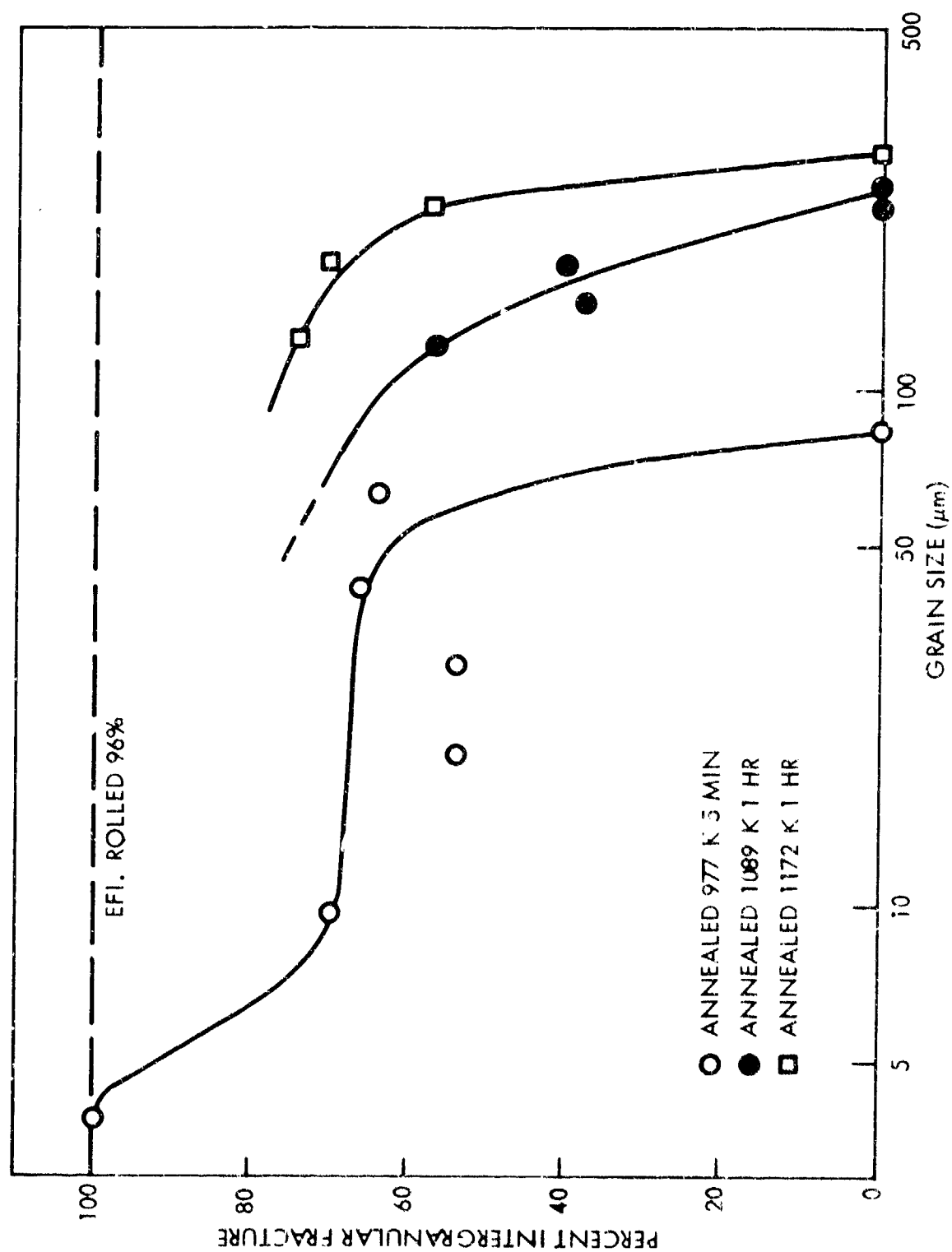


Fig. 19 Grain-Size Controlled Fracture Mode Transition for High-Purity Ingot Source Beryllium (EFI) Warm-Rolled 96% and Annealed at Various Temperatures

It was expected that an increase in the temperature of fracture above room temperature would significantly increase the tendency of the beryllium to fracture in an intergranular manner and also increase the grain size at which intergranular fracture occurred. A small increase in the latter parameter was observed in EFI (Fig. 20); however, in powder-source materials which have only about 10-percent intergranular fracture after cold work and recrystallization, no significant increase in the amount of intergranular fracture was observed up to 533 K, although the observed intergranular fracture became better defined at the higher temperature.

Fracture mode transitions for high-purity, HIP, powder-source beryllium are shown in Figs. 21-23. These materials show completely intergranular fracture for grain sizes below about 1- $\mu$ m diameter. Intergranular fracture at the larger grain sizes seems to be only in areas where little or no oxide particles occur, i.e., when recrystallized grains form inside the original beryllium powder particle boundaries. This is particularly true in the case of unworked HIP material where the amount of intergranular fracture is negligible and is seen only when multiple grains form inside a single powder particle and do not have oxide particles along their boundaries. These isolated regions, therefore, behave like ingot source and favor grain-boundary fracture.

### 5.3 MICROSTRUCTURAL OBSERVATIONS OF THE INITIAL STAGES OF FRACTURE

The above results have shown that fine-grain materials fracture predominantly along the grain boundaries. Previous work (Ref 2) on polished samples has indicated that grain-boundary sliding precedes and is probably responsible for intergranular fracture. However, to examine the microstructural events leading to grain-boundary fracture, recrystallized and partly recrystallized samples were deformed by cold-rolling at room temperature and examined by transmission electron microscopy. Specimens were examined in the areas containing the finest recrystallized grains for evidence of grain-boundary sliding or local deformation in boundary regions that could lead to grain-boundary fracture. The type of structure formed in a partly recrystallized ingot-source Be 0.19% Ti alloy after 15-percent reduction by rolling at room temperature is shown in Fig. 24.

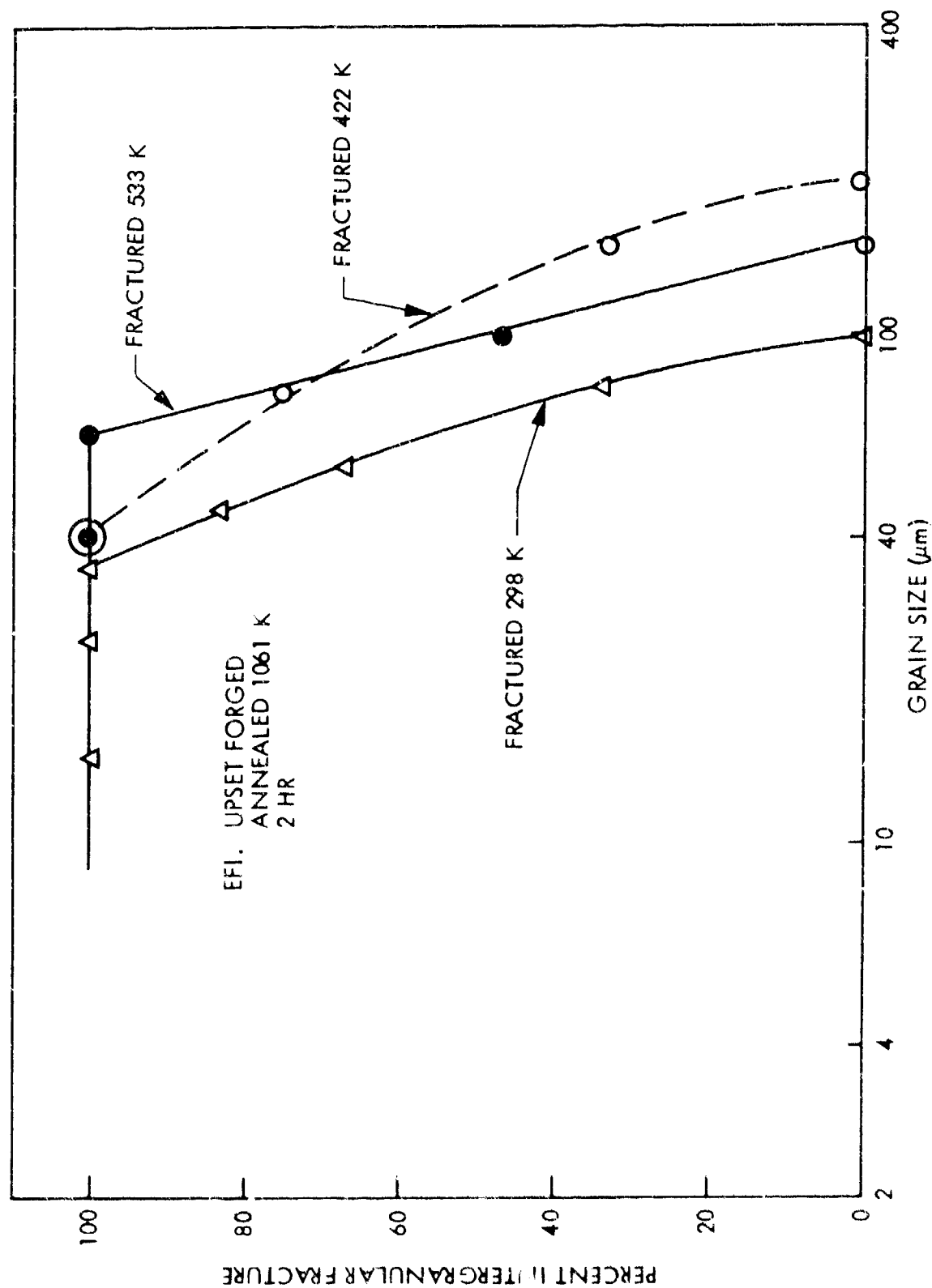


Fig. 20 The Effect of Temperature on the Grain-Size Controlled Fracture Mode Transition for High-Purity Upset-Forged, Ingot Source Beryllium (EFI)

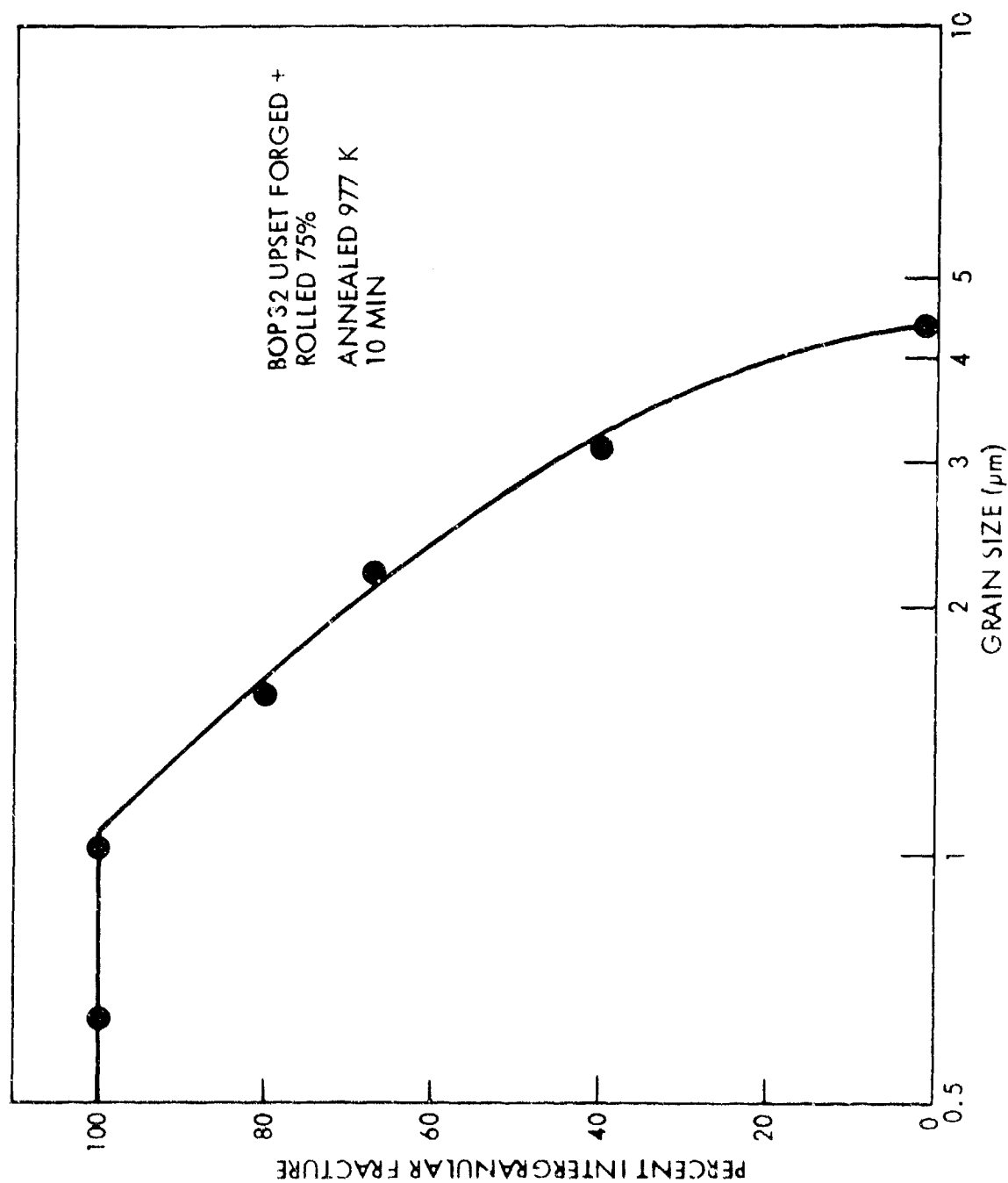


Fig. 21 Grain-Size Controlled Fracture Mode Transition for High-Purity HIP Powder Block (BOP 32)  
 After Upset-Forming and Warm-Rolling

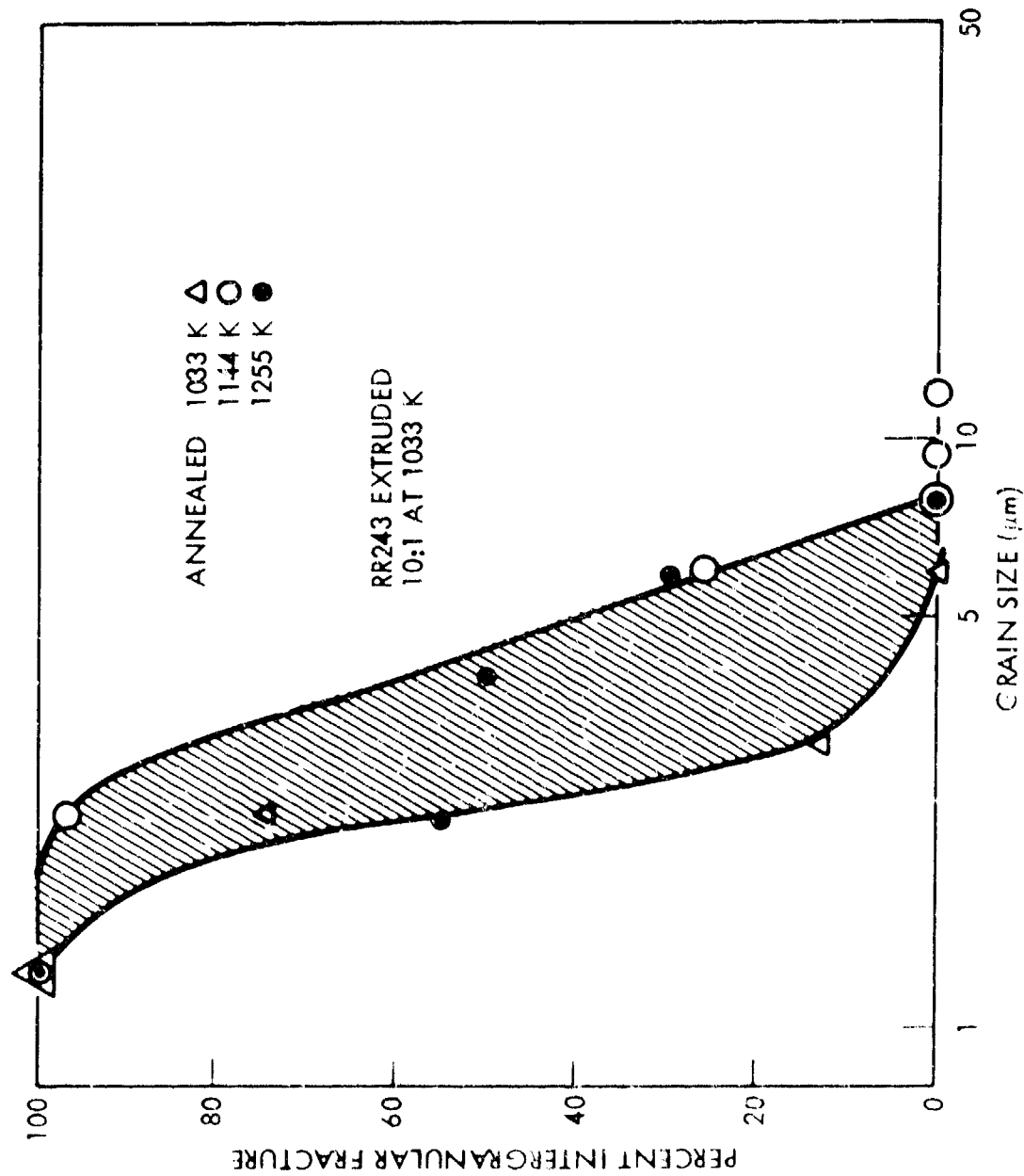


Fig. 22 Grain-Size Controlled Fracture Mode Transition for High-Purity HIP Beryllium RR243 After Extrusion and Annealing at Various Temperatures

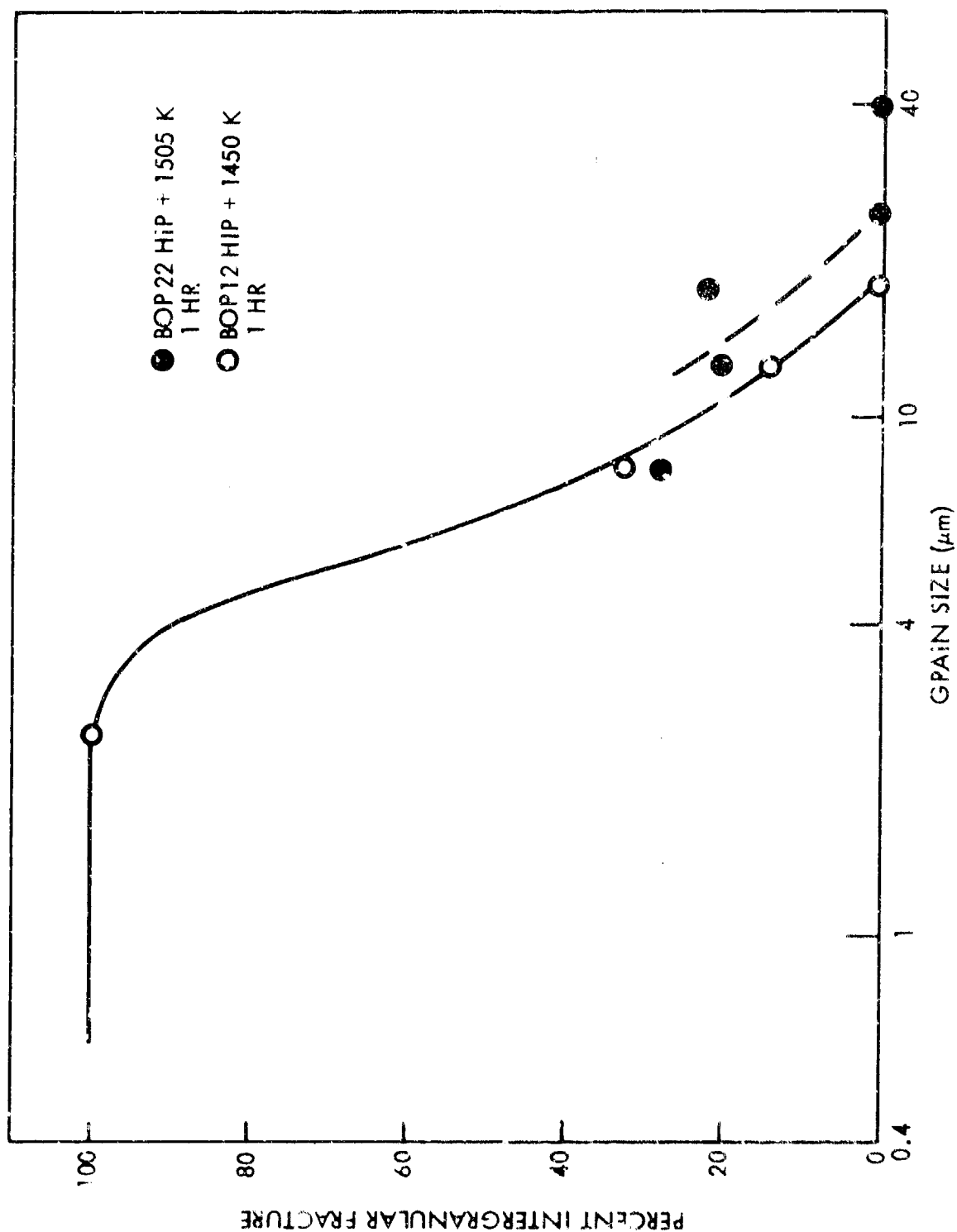




Fig. 24 Transmission Electron Micrograph of Cast Be 0.10% Ti, Warm Rolled 96%, Annealed 977 K 10 min, and Then Cold-Rolled 15%. A small crack has appeared on the grain boundary at A. Dislocation tangles at triple junction B may be evidence of sliding along one of the adjacent boundaries. Magnification 22,000x.

Before deformation, this area contained very fine ( $\sim 3 \mu\text{m}$ ) recrystallized grains of low-dislocation density. Deformation has produced a fairly uniform network of dislocations throughout the grains. A small ( $1\text{-}\mu\text{m}$ -long) crack has formed at a triple junction A and a tangle of dislocations at another triple-junction B may be evidence of the accommodation of grain-boundary sliding along one of the boundaries forming that junction and could be the precursor to fracture at that point.

Figure 25 shows the dislocation structure of a powder-source beryllium sample which has been upset-forged, rolled to a 75-percent reduction at 922 K, and then partly recrystallized at 977 K. The structure consists of a mixture of fine recrystallized grains in areas of low-oxide particle concentrations and even finer subgrains in areas of high-oxide concentrations. It should be noted that the central regions of both grains and subgrains are relatively free of dislocations. When a similar sample is deformed 10 percent at room temperature by rolling to simulate flow and fracture during tensile and impact testing, a high density of dislocations (Fig. 26) are produced in localized areas mainly around the boundaries of grains or subgrains formed during annealing. This concentration of dislocations along the grain boundaries is even more apparent in the thicker regions of the foil (Fig. 27) revealed by the 650-Kv microscope. These dislocation concentrations in grain-boundary areas are thought to indicate that plastic flow is occurring preferentially in these regions, probably by grain-boundary sliding leading to grain-boundary fracture. Two examples of grain-boundary fracture in the very early stages are shown in Fig. 28. At A, a grain-boundary crack  $0.025 \mu\text{m}$  wide and  $0.5 \mu\text{m}$  long can be seen with difficulty. A larger crack at B can be seen to lie near a grain-boundary triple junction. Deformation voids  $0.01 \mu\text{m}$  wide can be seen on oxide particles at A. The orientation of these voids can be used to determine the stress axis since in compression the voids are at particle-matrix interfaces at right angles to the compression axis (Ref. 5). The latter determined in this manner is shown in Fig. 28, and it can be seen that at least one branch of each grain-boundary crack and, in some cases, the heaviest grain-boundary dislocation tangles are on boundaries at approximately 45 deg to the stress axis along the lines of maximum shear stress. This is consistent with the idea that grain-boundary sliding is occurring and is the precursor to the observed grain-boundary fractures. An indication of the fracture process in coarser-grained material



Fig. 25 Transmission Electron Micrograph of High-Purity Powder Source Beryllium Alloy BOP 32, Upset-Forged, Rolled 75%, and Annealed 977 K 10 min. Structure shows a mixture of fine recrystallized grains and subgrains. Magnification 14,000×



Fig. 26 Transmission Electron Micrograph of Be 0.7% BeO (BOP 32), Upset-Forged, Rolled 75% at 922 K, Partially Recrystallized for 1 hr at 977 K, and Reduced 10% by Cold-Rolling. Heavy Concentrations of Dislocations are seen along many grain boundaries, but no cracks have formed in this region. Magnification 32,000 $\times$



Fig. 27 High-Voltage (650 kV) Electron Transmission Micrograph of a Relatively Thick Foil of BOP 32, 0.7% BeO, Upset-Forged and Rolled 75% at 922 K, Partially Recrystallized at 977 K for 5 min and Then Reduced 10% at Room Temperature. A heavy concentration of dislocation tangles along some grain boundaries can be seen. Magnification 75,000×



Fig. 28 Transmission Electron Micrograph of BOP 32, 9.7% BeO, Upset-Forged and Rolled 75% at 922 K, Partially Recrystallized 977 K 1 hr, and Deformed by Rolling 10% at Room Temperature. A small grain-boundary crack is visible at A, together with some faintly visible deformation voids on BeO particles which define the compression axis. A larger grain-boundary crack is visible at B. The cracks and many of the boundaries with a high density of dislocation tangles are approximately at  $45^\circ$  to the compression axis, i.e., along the lines of maximum shear stress. Magnification 20,000 $\times$

LOCKHEED PALO ALTO RESEARCH LABORATORY  
 LOCKHEED MISSILES & SPACE COMPANY, INC.  
 A SUBSIDIARY OF LOCKHEED AIRCRAFT CORPORATION

is shown in Fig. 29. This shows a fully recrystallized (grain size  $\sim 40 \mu\text{m}$ ) high-purity ingot-source material (EFI) after 14-percent cold reduction at room temperature. After a certain amount of plastic flow within the grains, a sharp grain-boundary crack has been nucleated, which then initiated a second crack, this time on a cleavage plane within the grain. It can be seen from Fig. 19 that a  $40\text{-}\mu\text{m}$  grain size in EFI fractures in both an intergranular and a transgranular manner.

#### 5.4 IMPACT RESISTANCE

The impact resistance of as-cast beryllium and dilute beryllium alloys is about 0.7 J. This can be increased about 40% by extrusion at 1033 K and partial recrystallization at 977 K (Fig. 30). However, if the extrusion is then rolled below its recrystallization temperature, the impact resistance can be increased to 2.4 J.

Similar results are seen when powder metallurgy extrusions are annealed (Figs. 31 and 32). After extrusion at 894 K, annealing is required to develop maximum toughness as shown for BOP 18, while after extrusion at 1089 K sufficient annealing occurs during extrusion to produce maximum toughness in the extruded condition. The effect of beryllium oxide content on the development of maximum toughness during annealing is shown in Fig. 32. As would be expected, the higher oxide material requires higher temperatures, and its peak toughness is less.

The effect of upset forging prior to rolling at 922 K produces a beneficial effect on the impact strength after annealing as shown in Fig. 33. This is presumably due to the greater anisotropy of the deformation and subsequent recrystallization when prior upset forging is used.

The impact transition temperature of a partially recrystallized powder-source beryllium extrusion, BOP 18, is shown in Fig. 34 to be about 200 K. The impact transition range of commercially produced cross-rolled sheet is shown for comparison. The commercial sheet has a poorly defined transition temperature which would appear to be about 600 K. The transition temperature in hcp metals, including beryllium, has



Fig. 29 Transmission Electron Micrograph of EPI Rolled 96%, Annealed 977 K, 1 Hour and Cold Rolled 14%. A sharp grain boundary crack has been initiated. Magnification 20,000x.

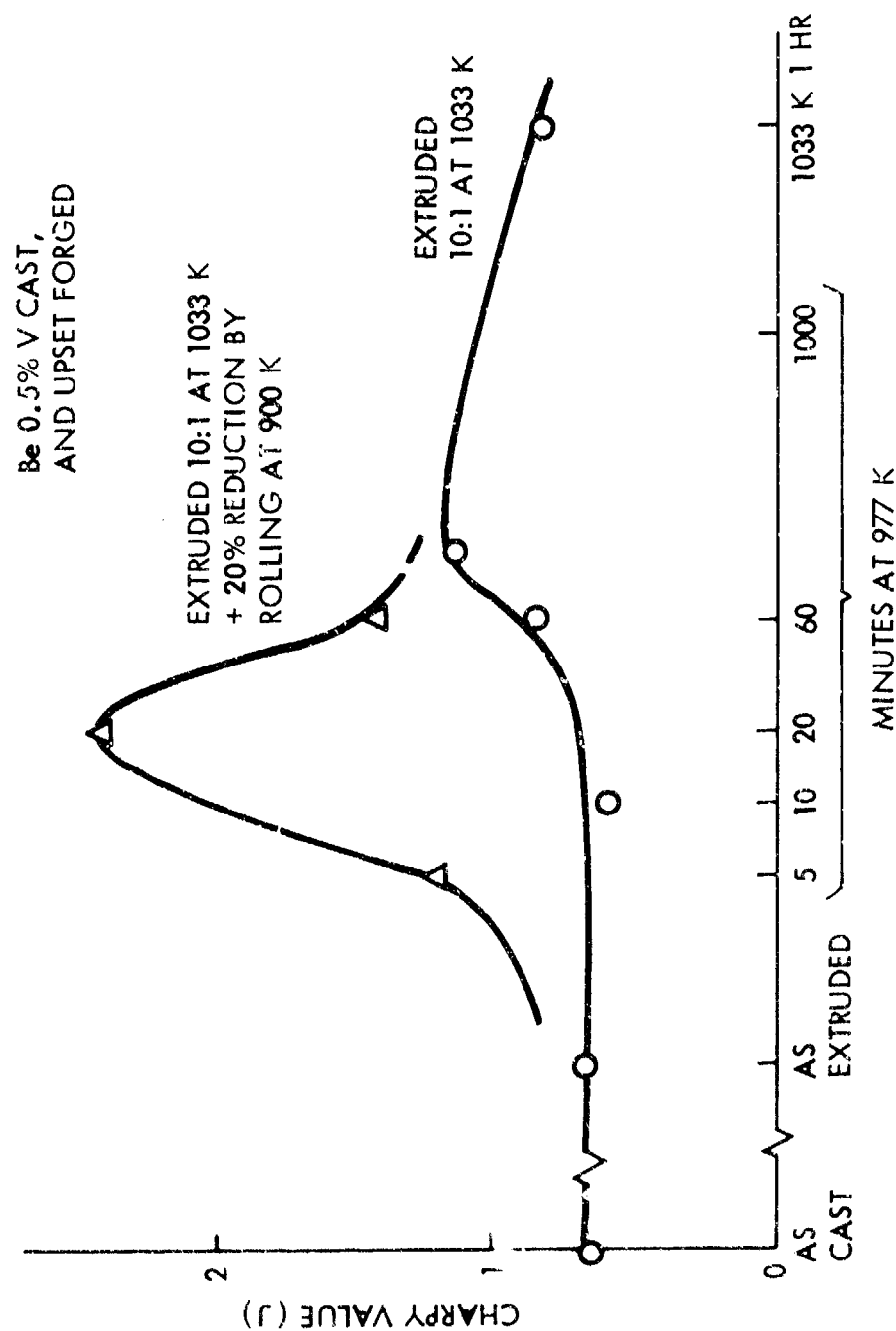


Fig. 30 Impact Toughness of Ingot Source Be 0.5% V, After Various Thermomechanical Treatments

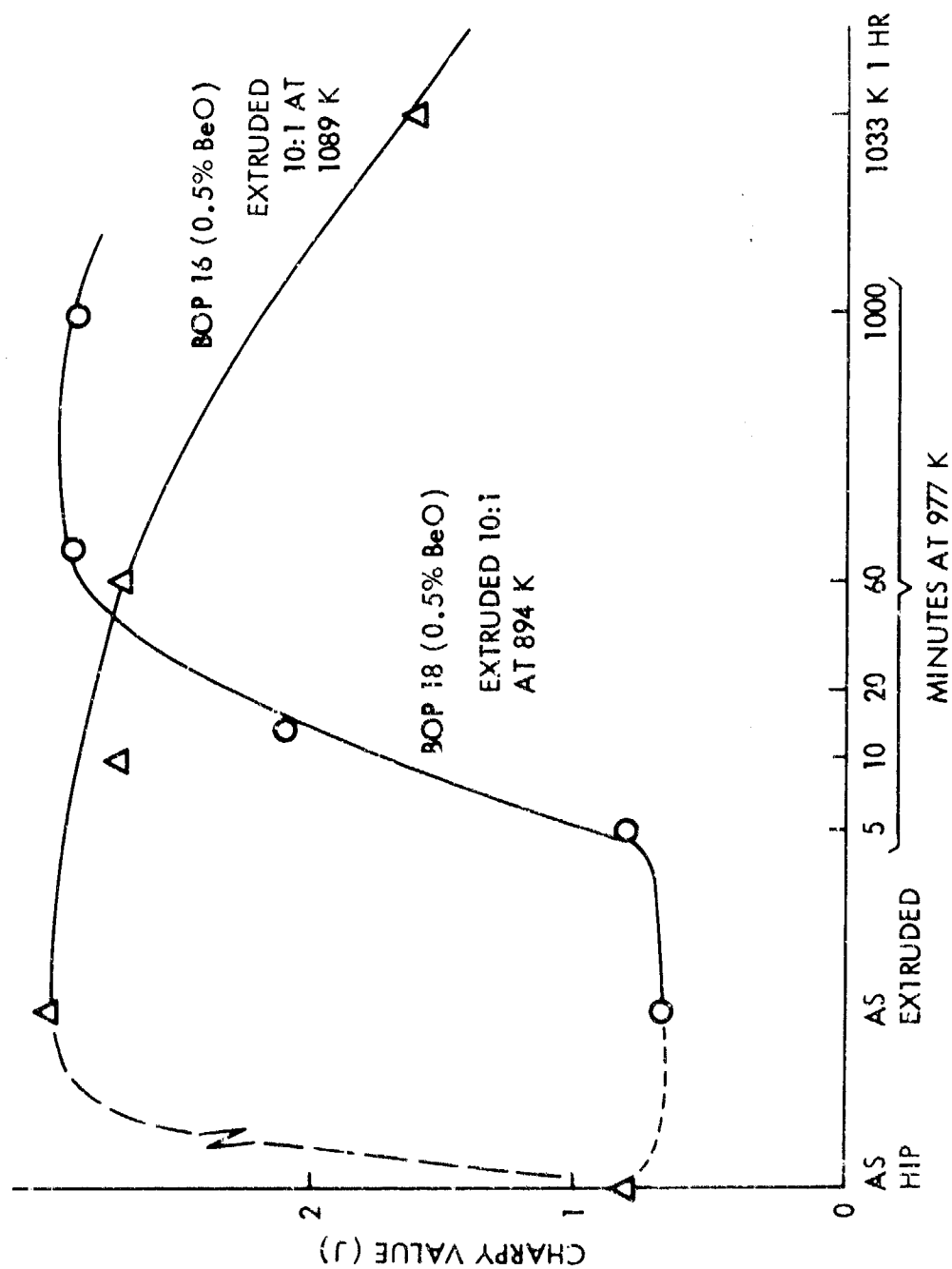


Fig. 31 Impact Toughness of High-Purity HIP Beryllium After Extrusion and Annealing

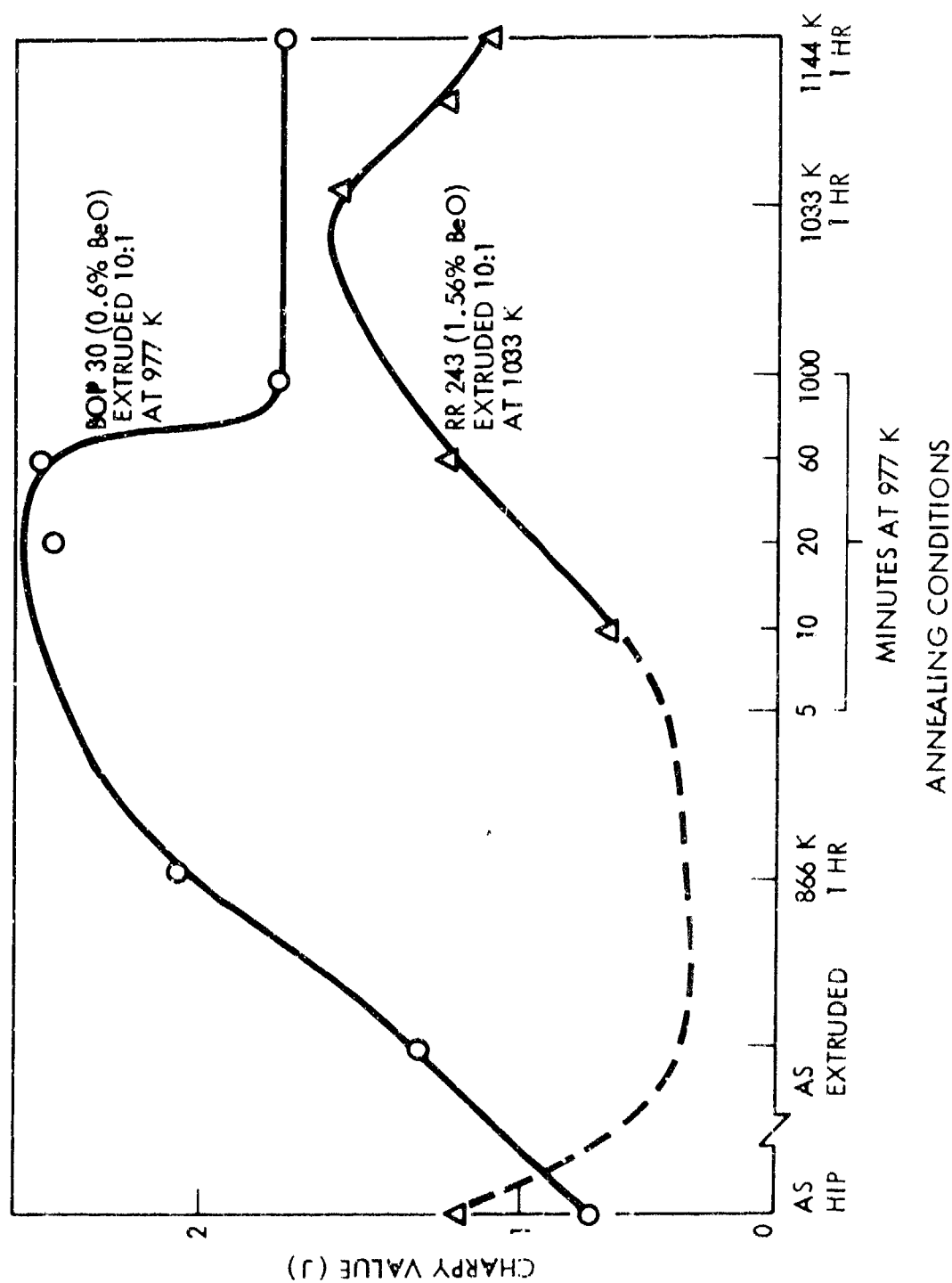


Fig. 32 Impact Toughness of High-Purity HIP Beryllium With Two Levels of BeO After Extrusion and Annealing

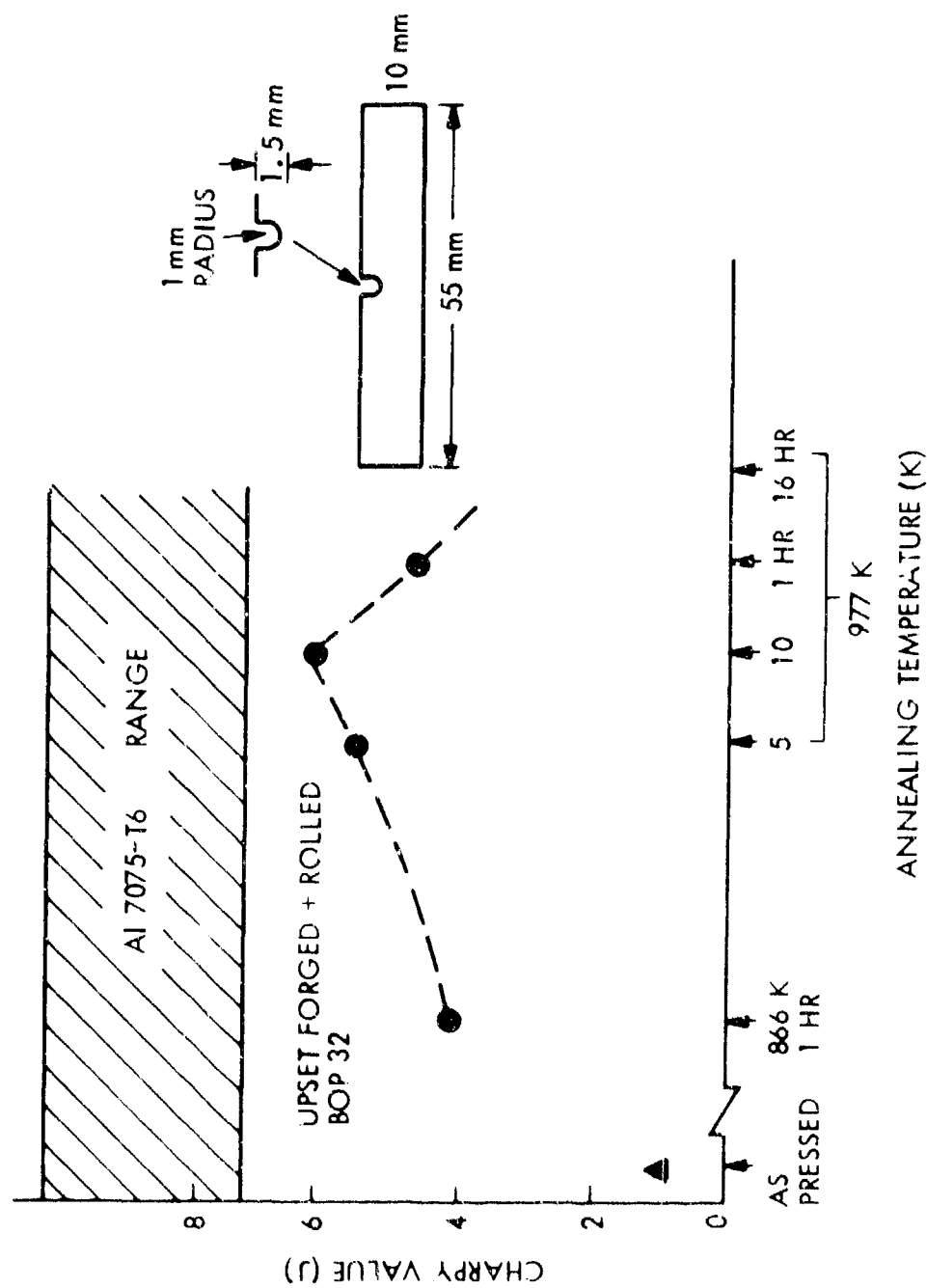


Fig. 33 Impact Toughness of High-Purity HIP Beryllium With Two Levels of BeO After Extension and Annealing

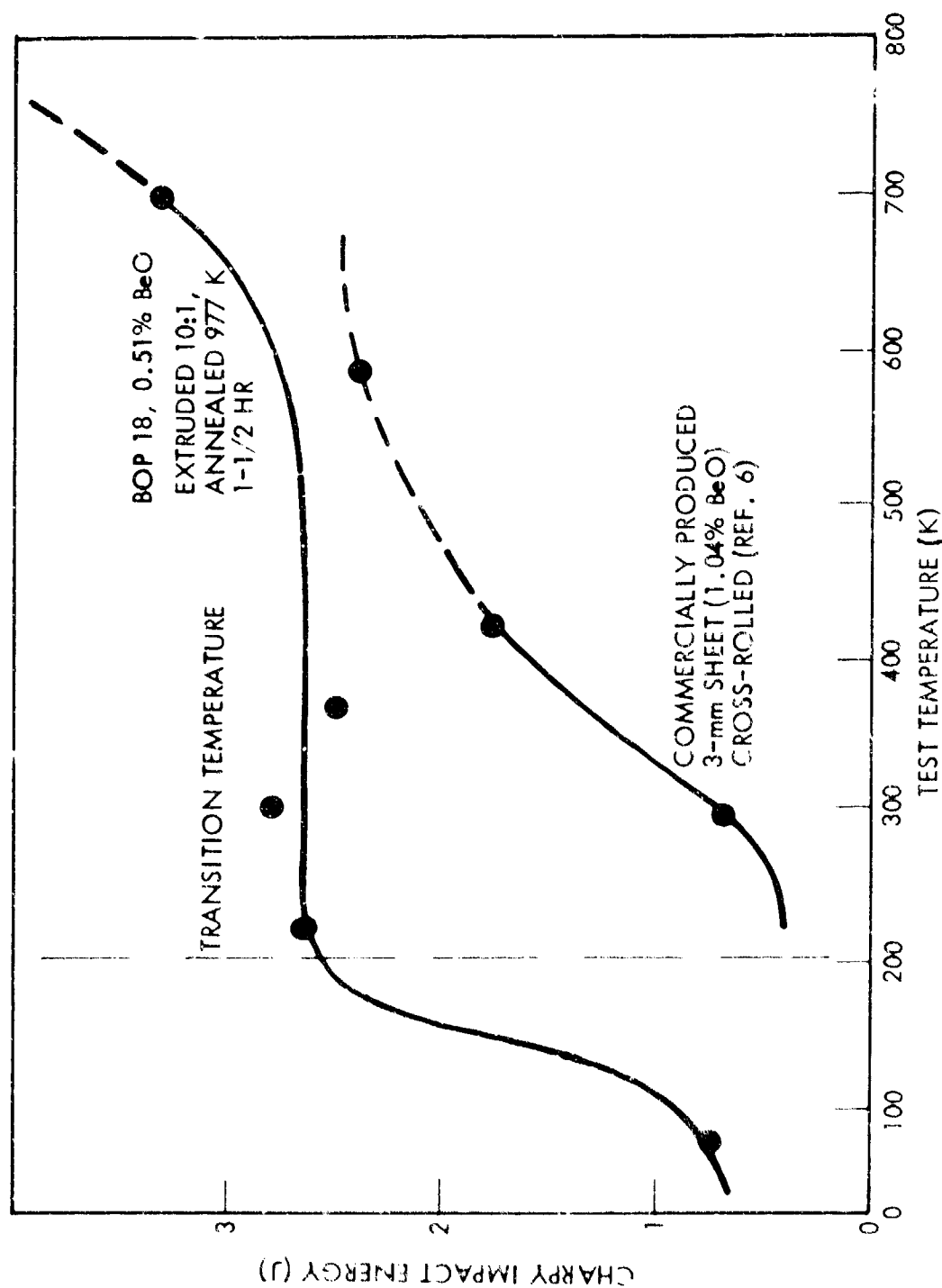


Fig. 34 Impact Toughness of High-Purity HIP Beryllium Block (BOP 32) After Upset-Forging and Warm-Rolling. The toughness of Al 7075-T6 tested with the same specimen design is shown for comparison

been predicted by Armstrong (Ref. 7) to be proportional to the square root of the grain size. Armstrong shows that if the data of previous investigators who determined transition temperature from ductility rather than toughness measurements are plotted in this way, the data extrapolate to a transition temperature of 200 K for very fine-grain sizes. The impact data plotted against  $d^{1/2}$  (Fig. 35) break down into three regions which are differentiated by the amount of dispersoid present. The higher the volume fraction of dispersoid, the lower the impact energy at a given grain size. The volume fraction of intergranular fracture of each sample is also indicated in Fig. 35, and this value will be used below to estimate the impact resistance of fully intergranular fracture at each grain size.

## 5.5 TENSILE PROPERTIES

Tensile testing of textured beryllium products can give misleading results since the strain-to-failure unlike toughness is extremely orientation-dependent, with the maximum tensile elongation being in the direction of maximum plastic flow during hot working. For this reason, tensile testing of extrusions was not performed, but an upset forging of a low-oxide, HIP block was made and tested in tension after various annealing treatments. The forging was upset six times in two directions with the third dimension remaining unchanged. Since there was zero metal flow in this third direction, it should be the direction in which tensile elongation is a minimum, and the tensile tests were carried out in this orientation. It has been demonstrated previously (Ref. 2) that the texture developed by upset forging is less than that normally found in a conventional hot-pressed block and that the variation in tensile elongation in an upset forging is about the same as that in the original billet. It has also been shown (Ref. 2) that the tensile elongation and bend angle of a casting forged in only two directions is not greatly dependent on testing direction and is expected to have about the same texture as a billet forged in three directions.

The mechanical properties of the upset forging are shown in Fig. 36. Compared to the "as-HIP" properties, there is an increase in strength, tensile elongation, and impact toughness. The peak ductility and strength occur after annealing at 1200 K, but the

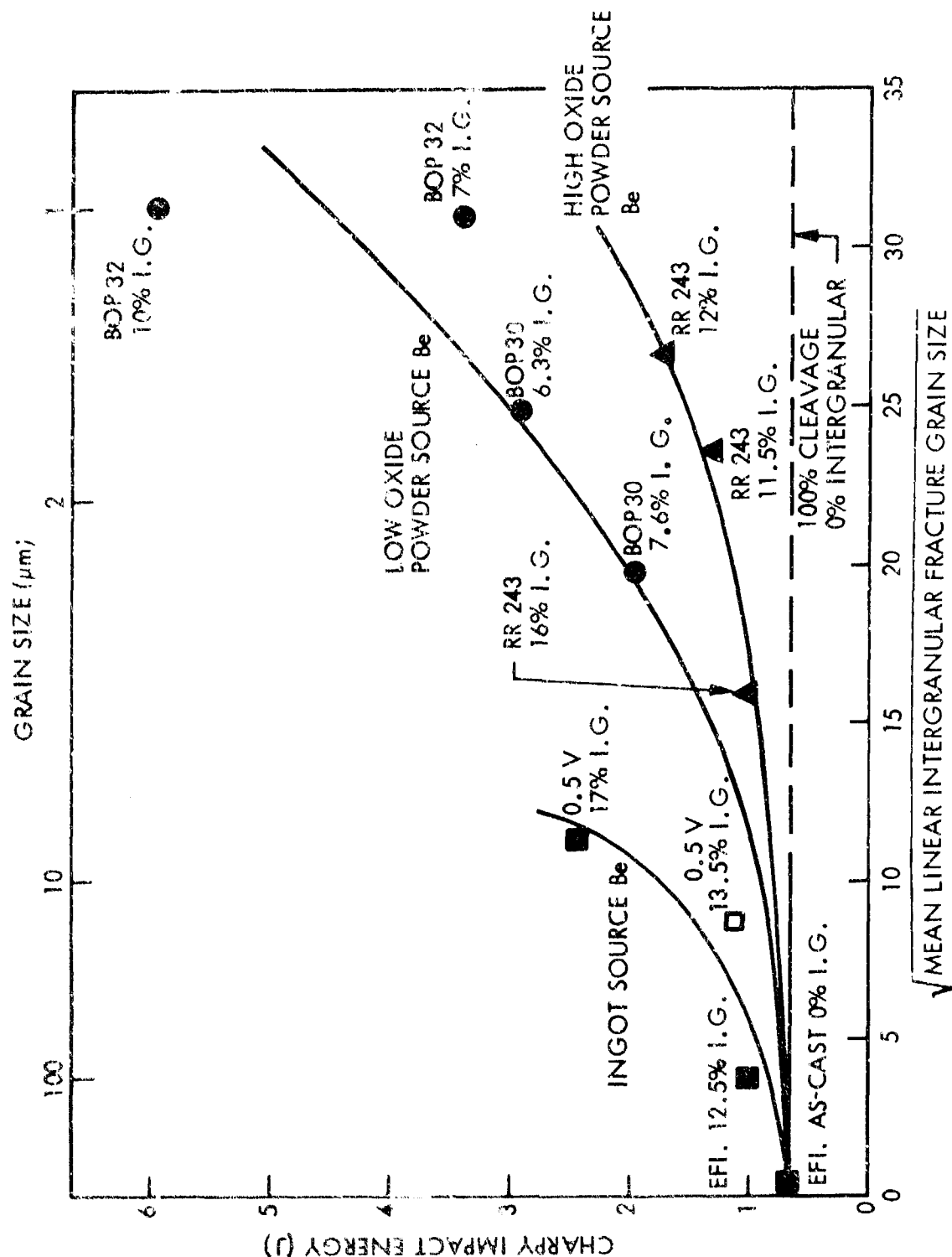


Fig. 35 Impact Transition Temperature for High-Purity HIP Beryllium (BOP 18) Extruded and Partially Recrystallized. The impact transition temperature of commercially produced sheet (Ref. 6) is shown for comparison

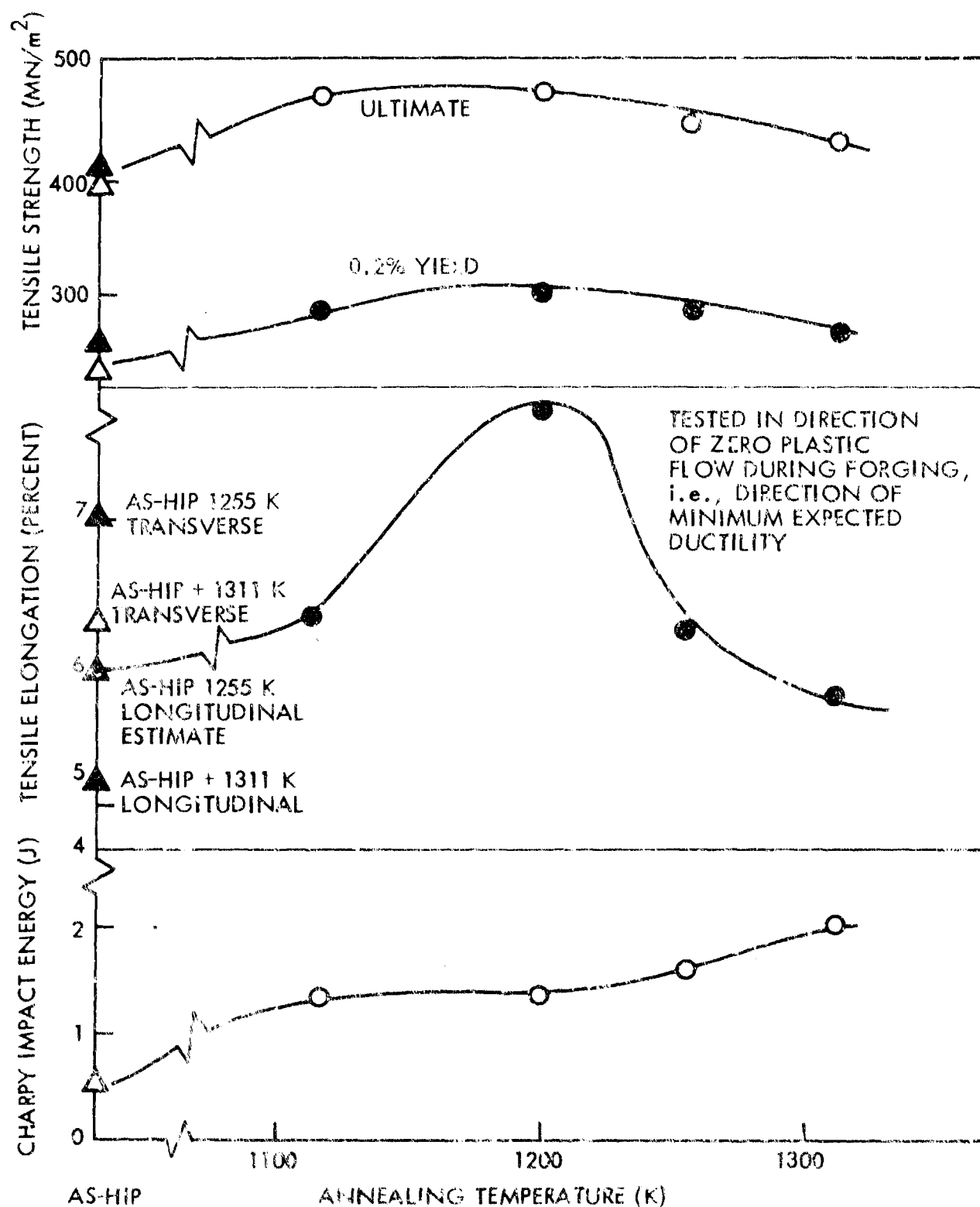


Fig. 36 The Effect of Grain Size on the Charpy Impact Energy of a Variety of Partially Recrystallized Beryllium Products. The amount of inter-granulation fracture (% I.G.) for each sample is shown

impact toughness is still increasing at the maximum annealing temperature tested (1300 K).

## 5.6 DISCUSSION

The above results indicate that when the grain size of beryllium is reduced below a certain value, the fracture mode changes from cleavage to intergranular. This transition is inhibited by dispersed particles such as BeO which occur in powder metallurgy products so that the transition is displaced to finer-grain sizes. It appears from previous work that even at room temperature grain-boundary sliding precedes intergranular fracture and that this additional slip mechanism allows beryllium to satisfy the Taylor-Von Mises criterion for homogeneous plastic flow which requires the operation of five independent slip systems. However, it is apparent that the change of fracture mechanism alone is only one of the factors contributing to toughness, since continued grain refinement of material that fractures in an intergranular manner produces significant increases in toughness (Fig. 35). Microstructural evidence indicates that in the toughest materials tested, there is considerable localized flow in grain-boundary regions before fracture occurs. It is logical to assume, therefore, that the beneficial effect of grain refinement is a result of the enhanced amount of grain-boundary flow or sliding that can occur before fracture is initiated.

Most of the materials examined in this work were only partially recrystallized or in advanced stages of recovery, and therefore were fractured only partially in an intergranular manner. However, it is possible to estimate what the toughness of materials fracturing in a completely intergranular manner at various grain sizes would be if two assumptions can be made. The first is that grain refinement has little effect on toughness if the specimen fractures by cleavage. For example, a high-purity casting with grains 10,000  $\mu\text{m}$  long has the same toughness (0.68 J) when the grain size is reduced to 200  $\mu\text{m}$  by upset forging (Ref. 2). It is only when the grain size is further refined and the fracture becomes intergranular that the toughness increases. Further support for this view is provided by beryllium block-tested in the as-pressed condition, where oxide particles are present on almost all grain boundaries and the fracture is over 95-percent cleavage.

These powder-source materials have about the same impact toughness as coarse-grained cast beryllium even though they have a grain size of only  $10\text{ }\mu\text{m}$ .

If the effect of grain refinement on the toughness of beryllium that fractures by cleavage is negligible and a constant value of  $0.68\text{ J}$  can be assumed, then the improvements in toughness illustrated in Fig. 34 are a result of the small volume of fine grains that fracture intergranularly. Since this volume fraction and its grain size are known, it is possible to calculate what the toughness would be at each grain size if the sample fractured with a 100-percent intergranular fracture. For example, the sample BOP 32 (upset-forged, rolled 75 percent and annealed at  $977\text{ K}$  for 10 min) has a measured impact value of  $5.95\text{ J}$  ( $4.46\text{ ft/lb}$ ). Since the fracture is 90-percent cleavage and 10-percent intergranular, the contribution of the component that fractures by cleavage will be  $0.9 \times 0.68 = 0.61\text{ J}$ . The remaining impact resistance contributed by the material that fractures intergranularly will be  $5.95 - 0.61 = 5.34\text{ J}$ . Since, in this case, this is only 10 percent of the total sample, if the entire sample fractured intergranularly at the same grain size, its toughness should be  $63.4\text{ J}$ . This calculation has been carried out for the data shown in Fig. 34 and is shown in Fig. 37. It can be seen that the projected impact values are considerably higher than high-strength aluminum alloys such as Al 7075 and at a grain size of  $1\text{ }\mu\text{m}$  approach the toughness of pure aluminum.

The next question is, How can a uniform fine-grain size of  $1\text{ }\mu\text{m}$  be achieved in beryllium without the high-oxide content formed when conventional powder metallurgy processes are used? One answer is that it can be done by the very rapid cooling of beryllium powder from the liquid state and consolidating it by techniques that do not allow grain growth. It is hoped that a program along these lines can be initiated in the near future.

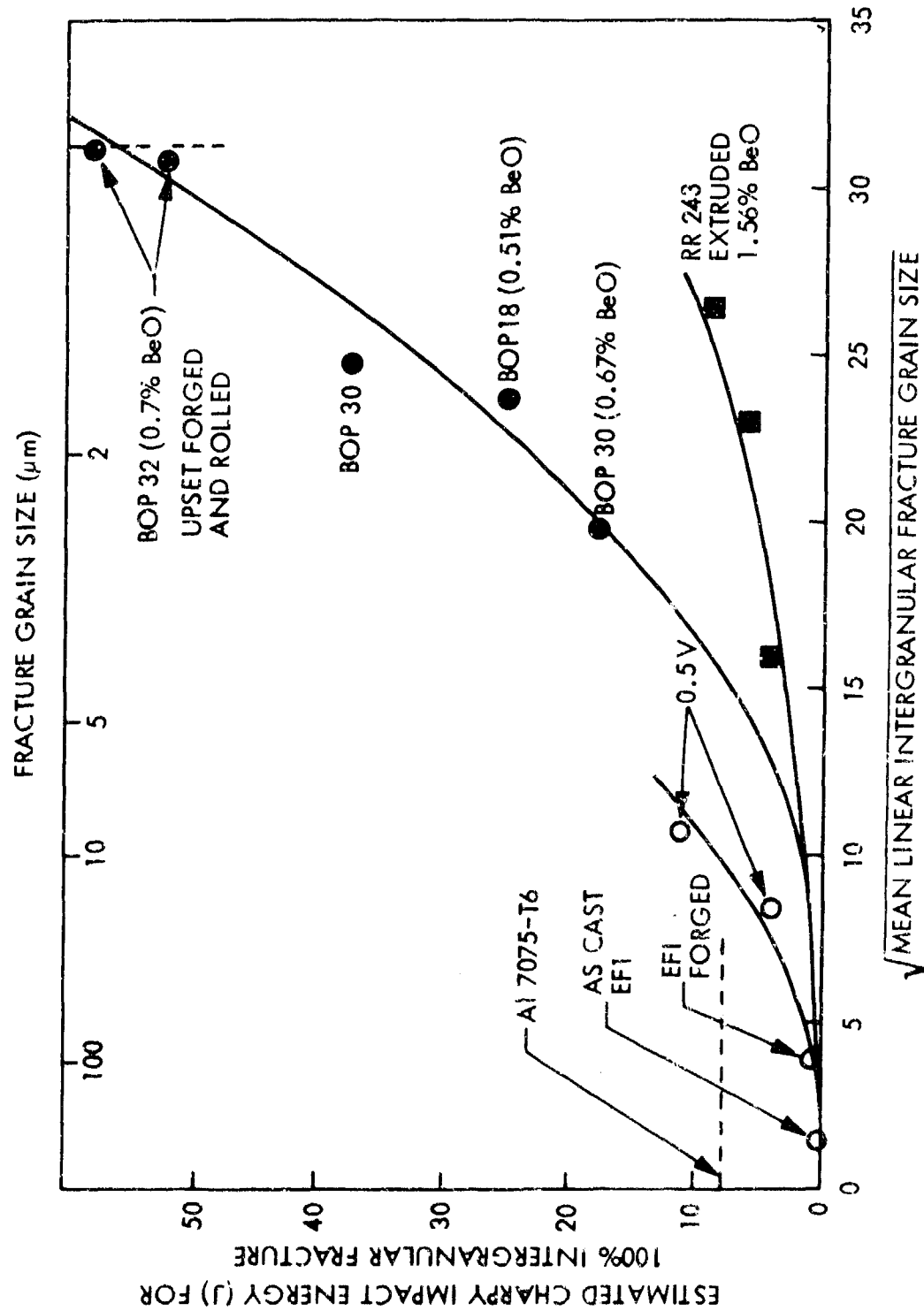


Fig. 37 The Effect of Annealing Temperature on the Strength, Ductility, and Toughness of Upset-Forged Beryllium

## Section 6 CONCLUSIONS

- (1) The impact toughness of high-purity, low-oxide, powder-source beryllium can be increased by thermomechanical treatments to a level not far below that of Al 7075-T6.
- (2) Optimum toughness occurs when the microstructure consists of very fine ( $< 4 \mu\text{m}$ ) recrystallized grains or subgrains which are on the threshold of recrystallizing in situ, and which fracture intergranularly.
- (3) There is a grain-size controlled fracture mode change in both powder-source and ingot-source beryllium. The change is displaced to finer grain sizes by oxide particles and texture.
- (4) There is potential for a considerable further improvement in the toughness of beryllium by the use of rapidly cooled powders.
- (5) To produce the finest grain size in beryllium for a given total reduction, a thermomechanical process should avoid any recrystallization before the final annealing treatment.
- (6) Recrystallization in heavily deformed beryllium occurs by the in situ transformation of subgrains to grains by the dislocation migration from grain interiors to grain boundaries.
- (7) Upset forging followed by annealing can produce increases in strength, ductility, and toughness.

Section 7  
REFERENCES

1. D. Webster, R. L. Greene, R. W. Lawley, and G. J. London, "Factors Affecting the Tensile Strength, Elongation and Impact Resistance of Low Oxide, Hot Isostatically Pressed Beryllium Block, Met. Trans., Vol. 7A, Jun 1976, p. 851
2. D. Webster and D. D. Crooks, Improved Beryllium Ductility Study, Contract N60921-74-C-0114, Final Report to Naval Surface Weapons Center, LMSC-D507268, Aug 1976
3. V. E. Ivanov, G. F. Tikhinskij, I. I. Papiro, I. A. Taranenko, E. S. Karpov, and A. S. Kapcherin, "Plastic and Superplastic Deformation of Fine Grained High Purity Beryllium," Proceedings of Fourth International Conference on Beryllium, London, 1977
4. D. Webster, R. L. Greene, and R. W. Lawley, "Factors Controlling the Strength and Ductility of High Purity Beryllium Block," Met. Trans., Vol. 5, Jan 1974, p. 91
5. D. Webster, "Grain Growth and Recrystallization in Thoric Dispersed Nickel and Nichrome," TMS. AIME, Vol. 242, Apr 1968, p. 640
6. Lockheed Missiles & Space Co., Inc., Final Report for Evaluation of Beryllium for Space Shuttle Components, LMSC-D159319, Contract NAS 8-27739, Sunnyvale, California, 1972
7. R. W. Armstrong, Acta Met, Vol. 16, 1968, p. 347